The Mars Observer Ka-Band Link Experiment

T. A. Rebold, A. Kwok, and G. E. Wood
Telecommunications Systems Section

S. Butman
TDA Technology Development

The Ka-Band Link Experiment was the first demonstration of a deep-space communications link in the 32- to 35-GHz band (Ka-band). It was carried out using the Mars Observer spacecraft while the spacecraft was in the cruise phase of its mission and using a 34-meter beam-waveguide research and development antenna at the Goldstone complex of the DSN. The DSN has been investigating the performance benefits of a shift from X-band (8.4 GHz) to Ka-band (32 GHz) for deep-space communications. The fourfold increase in frequency is expected to offer a factor of 3 to 10 improvement (5 to 10 dB) in signal strength for a given spacecraft transmitter power and antenna size. Until recently, the expected benefits were based on performance studies, with an eye to implementing such a link, but theory was transformed to reality when a 33.7-GHz Ka-band signal was received from the spacecraft by DSS 13. This article describes the design and implementation of the Ka-Band Link Experiment from the spacecraft to the DSS-13 system, as well as results from the Ka-band telemetry demonstration, ranging demonstration, and long-term tracking experiment. Finally, a preliminary analysis of comparative X- and Ka-band tracking results is included. These results show a 4- to 7-dB advantage for Ka-band using the system at DSS 13, assuming such obstacles as antenna pointing loss and power conversion loss are overcome.

I. Introduction

Theoretical studies in DSN telecommunications have shown that utilizing Ka-band (32 GHz) over X-band (8.4 GHz) on a spacecraft-to-ground link would yield a benefit of 3 to 10 times the telemetered data for a given spacecraft transponder weight, antenna size, and power allocation [1,2].[1] The enhancement comes from the increased antenna gain at smaller wavelengths, but it is reduced by other factors such as higher atmospheric noise, antenna performance deficiencies, and weather susceptibility at Ka-band.

Just as past transitions in the DSN from L-band (0.96 GHz) to S-band (2.3 GHz) and later to X-band yielded almost 20-dB improvements in link capacity, the transition to Ka-band appears to be the next logical step in the evolution of the DSN. The possibility of enhanced performance led to the proposal of a Ka-band link experiment

[1] R. L. Hortorr, ed., *Ka-Band Deep Space Communications*, JPL D-4356 (internal document), Jet Propulsion Laboratory, Pasadena, California, May 15, 1987.

to verify these studies [3] and to discover any obstacles that may prevent this gain from being achieved.

The experiment was taken up by the Mars Observer Project, originally on a best-effort basis and later with full commitment to carry on board the spacecraft a small Ka-band transmitter that could meet the proposed goals. As it became a reality, the Ka-Band Link Experiment (KaBLE) acquired the following specific objectives:[2]

(1) Verify the performance level of a Ka-band link versus an X-band link.

(2) Obtain 250-bit/sec telemetry data over the Ka-band link.

(3) Determine X-/Ka-band differential range to the spacecraft using the ranging code modulated on the X- and Ka-band carriers.

(4) Obtain experience in actual operations of a Ka-band link at a 34-meter antenna.

Mars Observer (MO) was launched on September 25, 1992. According to the KaBLE plan,[3] comparative X- and Ka-band observations would be performed weekly beginning with the Outer Cruise phase in January of 1993, when the spacecraft switched from the low-gain X-band only antenna to the high-gain antenna (HGA) and began transmitting both at Ka-band and X-band. Observations would continue beyond Mars Orbit Insertion to the completion of the Mars Observer mission in 1996. Due to the very weak signal level, the telemetry (TLM) demonstration could be performed only during the first two weeks of the experiment. Ranging was originally planned for the Mars opposition in January of 1995, but was later rescheduled to the period immediately following the telemetry demonstration. This was done for three reasons: first, to take advantage of signal strength due to relative nearness to Earth; second, to practice for a possible test of general relativity during solar conjunction starting mid-December 1993; and third, to diminish the chance of missing the ranging opportunity entirely, should the as-yet unproven KaBLE system on the spacecraft fail before the first Mars opposition in 1995.

This article summarizes the main accomplishments of the experiment, including the design of a Ka-band downlink, the implementation of a Ka-band tracking station at DSS 13, the successful acquisition of Ka-band telemetry and ranging data, and the routine carrier tracking performed from January 1993, to the unexpected loss of Mars Observer in August. A preliminary analysis explores some of the data processing that has been accomplished to relate the performance of Ka-band to the performance of X-band. Finally, future Ka-band performance studies in the absence of Mars Observer will be discussed.

II. Ka-band Link Design

A. Spacecraft Contribution

Mars Observer was equipped with a special 0.033-W transmitter and a 28-cm antenna to support the KaBLE with minimal impact on spacecraft power consumption and antenna design. The Ka-band primary reflector was actually the reverse side of the X-band subreflector, as seen in the spacecraft photograph and block diagram in Fig. 1. The Ka-band downlink was obtained from the 20-W X-band downlink using a 14-dB coupler and a times-four frequency multiplier. The output of the multiplier was physically routed via waveguide along a subreflector support leg to a focal-point feed on the Ka-band antenna. This design, evolved by Martin Marietta Astro Space (Astro), the spacecraft contractor, underwent several changes to increase the Ka-band power output from 0.012 W and to prevent overheating of the multiplier while in near-Earth cruise. The additional 4.4 dB of power margin proved to be very important in compensating for unexpected pointing loss and adverse weather conditions during the telemetry demonstration.

Table 1 derives the effective isotropic radiated power (EIRP) for Mars Observer at X- and Ka-bands, including nominal circuit losses and antenna pointing errors. Note that because of the difference in antenna diameters at X- and Ka-bands, the Ka-band antenna beam is actually wider than the X-band beam (1.3 deg at Ka-band versus 0.9 deg at X-band). Although the two antenna beams were about 0.4 deg off center, they were nevertheless aligned to less than 0.1 deg. As long as the high-gain antenna was pointed to Earth, the full X- and Ka-band power would be received. As it turned out, the high-gain antenna upon deployment was mispointed by 1 deg, resulting in a significant loss of received signal power at both frequencies. This will be discussed further in Section VI.

Because the Ka-band transmitter was essentially a times-four frequency multiplier, the modulation indices

[2] S. A. Butman and J. G. Meeker, *DSN Advanced Systems–Mars Observer Ka-Band Link Experiment Plan*, JPL-D 8799 (internal document), Jet Propulsion Laboratory, Pasadena, California, August 1991.

[3] Ibid.

for telemetry and ranging are four times higher at Ka-band than at X-band. For example, a modulation index of 45 deg at X-band becomes 180 deg (or pure carrier) when the signal frequency is multiplied by four. Spectra taken from Mars Observer during the electromagnetic emissions testing in Fig. 2 show the Ka-band signal that results from X-band telemetry modulations of 0, 44.8, 59.9, and 80 deg. As seen in the figure, the Ka-band spectrum at 44.8 deg (X-band modulation index) is nearly identical to the spectrum at 0 deg. This was particularly helpful during most of the KaBLE tracking, because it allowed the transmission of X-band telemetry from the spacecraft without suppressing the Ka-band carrier. For the telemetry demonstration, the optimum X-band modulation index for obtaining 250-bit/sec data at Ka-band was 59.9 deg, which multiplies to 239.6 deg (with the equivalent suppression of 60.4 deg) at Ka-band. However, it was necessary to gain the confidence of the mission designers and the approval of project management to operate the spacecraft in these modes.

B. Ground Station Contribution

The DSS-13 ground station is a prototype for a future DSN operational subnet of beam-waveguide antennas. Unlike Mars Observer, which was modified to carry a small Ka-band reference beacon, DSS 13 was designed mainly to focus on Ka-band performance. One of the reasons for building a beam-waveguide antenna was to allow locating the Ka-band front-end in the protected, easily accessed environment of the antenna's pedestal room. As will be seen, this feature also proved critical to the experiment's success during the adverse weather of the telemetry demonstration.

Figure 3 shows a high-level block diagram of the DSS-13 feed system from the antenna structure to the receivers. Table 2 shows the antenna gain/temperature (G/T) budget, which includes contributions from the maser, dichroic plate, antenna structure, atmosphere, and cosmic background radiation. A theoretical plot of G/T versus time (and elevation angle) is shown in Fig. 4 for a KaBLE pass in January 1993 (telemetry experiment) under weather conditions ranging from 0- to 90-percent worst-case likelihoods.

The complete link budget for the last day of the telemetry demonstration is shown in Table 3 for both X- and Ka-bands, using the EIRP derived in Table 1. This budget predicts a link margin of 2.1 ± 1.4 dB for telemetry reception. The 36-dB difference between the two downlinks becomes apparent when the total power–signal-to-noise ratio (P_t/N_0) at Ka-band is compared to X-band. Part of the task of the KaBLE is to normalize the results to form a fair comparison between the two downlink frequencies.

The above link budget depends to a large extent on spacecraft-to-Earth range, which varies considerably over the experiment. Figure 5 shows the expected variation in received Ka-band signal-to-noise ratio during the planned duration of the experiment. The dotted line at 29 dB-Hz indicates the minimum level required to obtain 250-bit/sec data at a modulation index of 60 deg; other marks indicate the minimum level for tracking the carrier under various spacecraft configurations. Even though carrier tracking could be performed throughout the 3-year experiment, the entire telemetry demonstration had to fit within a narrow 2-week window beginning the day after the high-gain antenna was activated. Further along, in January of 1995, an opportunity to obtain more data would have occurred, but only at a reduced 10-bit/sec rate.

III. Ground Station Design

The 34-m beam-waveguide antenna at DSS 13 was developed in two phases. In phase I, the antenna was designed, constructed, and rigorously tested for performance at X- and Ka-bands.[4] Transforming the antenna into an operational tracking station for KaBLE took place under Phase II using the requirements summarized in Table 4. Essentially, the station was required to simultaneously track the dual X- and Ka-band downlinks arriving from Mars Observer, demodulate and decode the telemetry data, and store the relevant tracking statistics for future analysis.

A block diagram of the KaBLE system is shown in Fig. 6. From a system level, the ground station can be broken into several subsystems: antenna, microwave, receiver, data acquisition, monitor and control, and frequency and timing. The highlights of each subsystem will be described below.

A. Antenna Subsystem

A primary concern for operating a 34-m antenna at Ka-band is the need for improved pointing accuracy. Whereas for X-band an accuracy of about 8 mdeg is sufficient, for KaBLE an accuracy of 2 mdeg was needed to limit pointing loss to less than 0.5 dB. In the past, pointing calibrations

[4] M. Britcliffe, ed., *DSS-13 Beam Waveguide Antenna Project, Phase I Final Report*, JPL D-8451 (internal document), Jet Propulsion Laboratory, Pasadena, California, May 15, 1991.

had been shown to correct errors to about 5 mdeg rms in a "blind" or open-loop mode.[5] The task of reducing the pointing errors fell to two approaches: (1) improvement of blind-pointing calibration models and (2) use of an automatic boresight algorithm known as AUTOBORE, which corrects pointing errors in real time.

To improve the blind-pointing model, calibrations were performed primarily on two radio sources lying in close proximity to the Mars Observer declination at the start of KaBLE. Since the antenna beams for X- and Ka-bands are not perfectly co-aligned, data were taken at both frequencies. The X-band calibrations, completed one month prior to the start, yielded very promising results of approximately 2.8 mdeg rms (at X-band).[6] However, several factors—including the length of time needed to collect data, last-minute corrections to the system, and bad weather—prevented the completion of a thorough Ka-band calibration. Instead, the initial KaBLE tracks utilized the X-band model. Refinement of the Ka-band pointing model was left to the period after the telemetry experiment, when the station was in a more stable configuration.

AUTOBORE performs a scan in both the elevation and cross-elevation axes, centered on the target, and uses measurements of signal level to determine and remove the pointing error. For natural radio sources, the signal-level estimate is simply the temperature of the source as provided by the total power radiometer (TPR). For spacecraft tracking, the parameter of interest is received carrier power (P_c). The boresight algorithm was modified to obtain P_c by reading carrier-to-noise ratio estimates (P_c/N_0) from the advanced receiver (ARX-II) and multiplying these by noise temperature estimates (N_0) from the TPR.

During normal operations, both the pointing model and the boresight algorithm were employed. A typical worst-case acquisition scenario (during heavy overcast or when the Ka-band signal was very weak) was handled in several steps: (1) the antenna was pointed using the Ka-band pointing model, (2) the ARX-II acquired X-band, (3) automatic boresighting removed X-band errors, (4) the second ARX-II acquired Ka-band, (5) automatic boresighting removed Ka-band errors, (6) the antenna tracked the target with corrected pointing offsets, and (7) automatic boresighting removed errors every hour. When the signal was strong, acquisition of Ka-band usually took place in step 2.

B. Microwave Subsystem

The microwave subsystem at DSS 13, as shown in Fig. 3, takes advantage of the pedestal room layout to allow switching among different feed packages arranged in a ring around a rotating ellipsoid reflector. The feed package used for KaBLE consists of an X-/Ka-band dichroic plate, an X-band high-electron mobility transistor (HEMT) low-noise amplifier (LNA), and a Ka-band maser. The main accomplishments in this area were the fabrication of the dichroic plate and development of JPL's first Ka-band cavity maser.

The X-/Ka-band dichroic plate is essentially transparent at Ka-band and reflective at X-band. It was designed primarily to study performance at the DSN-allocated Ka-band frequencies of 32 GHz (to receive) and 34 GHz (to transmit), and only secondarily for KaBLE. The KaBLE downlink of 33.66 GHz fell at a rather poor location between the two well-matched bands. Thus, out of the 11 K that the dichroic plate contributes to the KaBLE Ka-band system noise temperature, perhaps 6 or 7 K would be eliminated at a more optimal frequency.

Probably the most critical task of the KaBLE was the construction of JPL's first Ka-band cavity maser. To maximize the sensitivity of the system at Ka-band, an ultralow-noise amplifier (ULNA)—a cavity maser with a cryogenically cooled feedhorn, waveguide components, and a postamplifier—was developed with a noise temperature of 5 K at the feedhorn aperture. The maser itself was cooled to 1.6 K with a double-Dewar, open-cycle cryogenic system. The system noise temperature at Ka-band using the ULNA was about 41 K on a clear day. This is somewhat higher than the requirement in Table 4 of 33 K, mainly due to the extra contribution from the dichroic plate. Figure 7 shows a cross section of the maser cryostat with the actual maser embedded in the inner Dewar. The design and performance of the KaBLE ULNA are described in detail in a separate article [4].

For X-band downlink reception, a simple HEMT LNA was installed, yielding a system noise temperature of about 37 K. One additional LNA, a Ka-band HEMT with a system noise temperature of 65 K, was used to back up the maser.

[5] L. Alvarez, "Pointing Accuracy Measurements," in *DSS-13 Beam Waveguide Antenna Project, Phase I Final Report*, JPL D-8451 (internal document), Jet Propulsion Laboratory, Pasadena, California, May 15, 1991.

[6] L. Alvarez and C. Racho, "Estimated DSS-13 Ground Antenna Pointing Performance During the KaBLE Telemetry Demonstration," Interoffice Memorandum 3324-93-032 (internal document), Jet Propulsion Laboratory, Pasadena, California, March 18,1992.

C. Receiver Subsystem

The receiver subsystem for both X- and Ka-band consists of an RF–IF downconverter, a fiber-optic transmission link from the pedestal room to the control room, IF distribution in the control room, and an ARX-II—a digital receiver used for prototyping advanced receiver concepts (Fig. 6). For the X-band path, downconversion is performed using the 8.1-GHz first local oscillator (LO) that is a standard for the DSN. For the Ka-band path, a two-stage downconversion is employed, mixing the incoming 33.7-GHz nominal downlink signal with a 25.2-GHz first local oscillator followed by an 8.2-GHz second local oscillator. All local oscillators are coherent with the station frequency and timing subsystem (FTS).

It was found early on in the design of the system[7] that the Doppler jerk (rate of acceleration) from the spacecraft while in orbit around Mars, together with the weak 10-dB-Hz signal level expected, would (at Ka-band only) exceed the tracking capability of any third-order phase-locked loop, including that of the ARX-II. To remedy this problem, a device known as the Doppler tuner was developed to remove the predicted Doppler profile from the Ka-band signal prior to the ARX-II.

At the heart of the Doppler tuner lies a programmable oscillator (PO) designed by the Goldstone Solar System Radar Group (Fig. 8). The PO works in conjunction with a synthesizer, accepting time-coded Doppler predict files and adjusting a reference to the synthesizer to match the Doppler frequency at any given time. The Doppler correction converter, after an initial upconversion, mixes the IF with the output of the synthesizer, thus providing a 300-MHz fixed-frequency Ka-band IF to the ARX-II.

To fulfill KaBLE's requirement for two advanced receivers, a second receiver, intended for permanent location at DSS 13, was built. Known as TP-13 (for DSS-13 telemetry processor), this receiver was equipped with faster signal-processing and monitor hardware, making it the receiver of choice for Ka-band. In terms of function, the two receivers are essentially interchangeable and can be used to back up each other: in the event of a hardware failure, the functioning unit would be used for Ka-band.

Finally, one extra level of redundancy was provided by the multi-tone tracker (MTT), a digital receiver particularly suited for KaBLE. Because of its multichannel capability, the MTT can track X- and Ka-bands simultaneously, and also use the phase of the X-band carrier to aid the tracking of the Ka-band carrier. This technique takes advantage of the coherent, factor-of-four relationship between the X- and Ka-band downlink frequencies, allowing the detection of very weak Ka-band signals and tracking with very narrow loop bandwidths. Carrier aiding is even more effective than the Doppler Tuner in removing Doppler from the Ka-band signal, because the strong, easily tracked X-band carrier offers real-time information on what the signal is actually doing, rather than what it is predicted to do.

[7] T. Rebold, "Tracking KaBLE Doppler Accelerations," Interoffice Memorandum 3393-91-167 (internal document), Jet Propulsion Laboratory, Pasadena, California, November 11, 1991.

D. Data Acquisition Subsystem

Most of the remainder of the ground subsystem falls under the broad category of data acquisition. Here the relevant link parameters are measured and recorded for future analysis. The instruments included in this subsystem are the TPR for measuring system noise temperature; the water vapor radiometer (WVR) for measuring the quantity of water in the atmosphere; the weather station; and the data handling terminal (DHT) for measuring telemetry performance, displaying data from the other instruments, and recording all KaBLE-specific data to disk.

The TPR operates together with the microwave switch controller (USC) in the Microwave Subsystem to perform calibrated system noise temperature (SNT) measurements on a continuing basis during a track. Measurements of the total IF noise power are made with two HP436A power meters—one each for the X- and Ka-bands. A local terminal reads these measurements and converts them to SNT values at a rate of once per second, based on a transfer function derived from a previous calibration.

Calibrations can be initiated by operator command at any time during a track. A total of six calibrations are performed with the antenna at zenith before and after a track, and the results are averaged to form a single calibrated transfer function. During each calibration, the TPR measures the total IF noise power while the USC switches the maser input from sky, to noise diode, to ambient load, to both noise diode and ambient load. The measurements are then converted into a transfer function (SNT as a function of total noise power) and an estimate of system nonlinearity.

The WVR is a small, stand-alone package positioned some distance from the antenna, which calculates the presence of atmospheric water in vapor and droplet form along the antenna beam by measuring noise levels at 20.7 and 31.4 GHz. It consists of a platform with a small feedhorn and mirror assembly that can observe any point in the sky

with a beamwidth of 7 deg. It performs periodic tipping curves from zenith to 20-deg elevation and, when provided with pointing predicts, tracks along the line of sight of the 34-m antenna.

Data collected by the WVR can be used to understand the Ka-band tracking results by indicating the condition of the atmosphere in the direction the antenna is pointing. When a cloud passes overhead, for instance, the WVR will show the increase in sky temperature, from which the expected drop in Ka-band signal level can be estimated. Eventually, the WVR will be used to remove atmospheric effects, such as fluctuating path length delays, from the tracking data.

The weather station samples and records a range of meteorological parameters, including temperature, humidity, wind speed, and wind direction. Like all the instruments in this subsystem, data are stored locally and routed through monitor and control to a central storage device: the data handling terminal.

During operations, the DHT is routinely monitored for insight into the state of the downlink. Such data types as carrier-to-noise ratio, SNT, antenna elevation angle, and wind speed can be displayed simultaneously versus time on a single monitor. In addition, for tracks demonstrating Ka-band telemetry reception, the DHT calculates and displays the telemetry bit-error rate (BER) of the Ka-band data using the virtually noise-free X-band data for reference. Most data arrive at the DHT through the station data recorder (SDR), a gateway terminal that serves to back up data archiving and relieve some of the real-time load from the DHT. A second interface provides the DHT with two channels of 250-bit/sec telemetry data from the receivers' convolutional decoders.

E. Monitor and Control Subsystem

Tying all subsystems together into an operational system with a high degree of flexibility is the task of the monitor and control (M&C) subsystem. The main strength of the DSS-13 M&C subsystem is its user interface, a window-driven software display configured by the operators rather than the developers. The window approach provides both a high-level view of the entire system and a detailed configuration table for each individual subsystem. In this approach, flexibility is guaranteed: When a new project is assigned to the station (such as KaBLE), a new set of displays are developed by the operators for the particular subsystems used by a project. Then, at the start of a new track, the appropriate display package is loaded into memory and configuration is begun. Naturally, this approach lends itself well to automation, and an effort is under way to allow automated remote operations of the station after normal shift hours.

The M&C subsystem currently runs on a 486-platform. Eventually, the entire software package will be transferred to a Sun workstation. Interfacing to the other subsystems is provided by a local area network (LAN), a token bus easily modified to include new subsystems as they are added to the system. Each subsystem's host computer taps into the LAN through a special board plugged into its chassis, and a driver for handling real-time commands is loaded into the host computer's RAM at power-up.

F. Frequency and Timing Subsystem

KaBLE was able to benefit from the maturing fiber-optic technologies on two fronts. In the area of frequency and timing, all of the sensitive reference frequency distributions were made with fiber. In fact, even though DSS 13 has a hydrogen-maser frequency standard, the prime standard for the station is located about 20 miles away in the control room of Signal Processing Center (SPC)-10. With fiber optics, the degradation of the standard over that distance is practically immeasurable. Distribution of the 100-MHz first local oscillator to the downconverters in the pedestal room is also performed using fiber. Even many instruments in the control room are now given fiber-optic frequency references. The result is an exceedingly stable frequency reference for the entire system, which happens to be coherent to SPC-10 as well.

The second use of fiber optics is in the transmission of broadband IF signals. A fiber line connecting the pedestal room to the control room improves upon the instability normally obtained from coaxial cable. But the real advantage came with the installation of an IF link from DSS 13 to SPC-10, allowing use of the DSS 13 X-/Ka-band front-end with the two Pioneer-10 receivers located at SPC-10, where they could be interfaced to the ranging and Doppler equipment. Thus, for the modest cost of four fiber-optic transducers, a number of valuable possibilities were enabled, including a backup telemetry string and a viable Ka-band ranging system.

IV. Testing

System testing for KaBLE began in July of 1992 and continued in blocks as individual subsystems were installed

or upgraded all the way to the start of the telemetry demonstration in January of 1993. Antenna time for KaBLE was sandwiched between the numerous other tasks supported by DSS 13, including the High Resolution Microwave Survey (HRMS) and the Array Feed Project.

System performance tests, covering the period from July to August of 1992, focused on the basic functions of the KaBLE system: verification of system linearity and radiometric measurements, acquisition and tracking of frequency-ramped carriers, and acquisition and decoding of telemetry data. An important side benefit of these tests was getting acquainted with subsystem peculiarities and bringing software bugs to the surface for troubleshooting and repair.

A series of tracks were performed in August using the Voyager and Magellan downlinks as test signals. These tracks, although X-band only, were close approximations to a KaBLE track in terms of Doppler rate, signal level, and antenna pointing. As the first tracks with real signals, they were very helpful in proving not only receiver and telemetry performance but also the accuracy of the predict generation software. In addition, they offered the first opportunity to verify the AUTOBORE pointing correction algorithm on spacecraft signals. As the experiment start date approached, tracks of Mars Observer at X-band over the low-gain antenna were repeated for the operations exercise approximately once every two weeks.

Among the problems that arose during testing, one of the more serious was the lack of proper subsystem interfacing over the station LAN. This resulted in subsystem crashes whenever a complex task was performed, in particular during the AUTOBORE sequence where the antenna monitor and control (AMC) configures and reads data from the advanced receiver and the total power radiometer at the same time. Since most of the subsystems were able to function perfectly well in stand-alone mode, it was not a fatal problem. But to get the antenna to boresight properly, a great deal of time was invested in debugging the interfaces.

Shortly after the installation of the Ka-band ULNA in late November, a gain oscillation was observed in the Ka-band path, with a period on the order of 2 min and an amplitude of about 5 K. The source of the oscillation, first thought to be the ULNA, was later isolated to the downconverter. It turned out that a temperature controller in the Ka-band downconverter assembly had, due to a power glitch, reset its control values to a stored default, causing the temperature, and hence gain, in the assembly to oscillate. (As seen in Section VI, the maser gain and noise temperature were also prone to fluctuate.)

All this had the effect of delaying quality antenna calibrations at Ka-band until several days prior to the start of the experiment. By then the weather was already routinely cloudy and wet, and good data could not be taken at Ka-band. As a result, the X-band pointing model was used during the first several KaBLE tracks until accurate calibrations could be made at Ka-band. Because of this, pointing losses at Ka-band grew rapidly between boresights—about 0.75 dB/hr on average.[8]

V. KaBLE Operations

A. Predicts Generation and Delivery

The task of routine spacecraft tracking at an R&D station like DSS 13, not to mention the unique requirements of tracking at Ka-band, prompted the development of a special predicts-generation software package known as PG-13. The basic requirements for PG-13 were to provide time-tagged antenna pointing predicts accurate to 0.1 mdeg (to be consistent with the 2-mdeg overall budget) and X- and Ka-band frequency predicts accurate to within 100 Hz (to fall within a convenient acquisition range of the ARX-II).

Testing of PG-13 was performed both by comparing its output with Network Operations Control Center support system (NSS)-derived predicts and by measuring predict errors during test tracks of Voyager, Magellan, and Mars Observer. Eventually the level of accuracy was refined well beyond requirements: antenna predicts to much less than 0.1 mdeg and frequency predicts to about 1-Hz accuracy. This level of accuracy requires close attention to detail and the maintenance of a database of station locations, planetary ephemeris, spacecraft trajectory, spacecraft ultrastable oscillator (USO) frequencies, and uplink exciter ramps, which must be updated on a regular basis.

In the case of one assembly, the Doppler tuner, the frequency predicts provided by PG-13 were transformed into a series of Chebychev polynomial expansions using a standard algorithm [5]. Another assembly, the multi-tone tracker, was provided predicts directly by its developers.

The delivery of predicts from JPL to the DSS-13 M&C was nearly instantaneous over the NASA Science Internet (NSI) connection to Goldstone. From there, predicts were either downloaded by the station operator to the destination subsystem or typed into the appropriate window display on monitor and control.

[8] L. Alvarez and C. Racho, op. cit.

B. Station Operations

During a track, station operations were governed by a sequence-of-events (SOE) file, listing initial station and spacecraft configurations as well as the key events for the track. A typical track consisted of configuring the station for KaBLE, downloading predict information to the appropriate subsystem, performing noise temperature precalibrations at zenith, acquiring the signal, boresighting the antenna, and occasionally reacquiring the signal during uplink transfers with the spacecraft. After the track, data files were transferred from the data handling terminal to M&C, where they could be accessed over Internet from JPL.

The goal was for system operations to be under the control of one person. Ideally, all commands would be sent from M&C over the station LAN to the various subsystems. In practice, however, actual operations were more labor intensive than planned because of the many problems associated with a new system; typically, these operations required the attention of two operators and the experiment engineer. Just about every subsystem had its bad days, resulting in some unique station problem that had to be debugged before the track could proceed. Until the problematic AMC/M&C interface was refined, antenna boresights were routinely commanded from the local AMC terminal in the pedestal room. Fortunately, the requirement that each subsystem be able to operate locally made the system flexible enough to handle most contingencies.

Even so, KaBLE operations sometimes presented unusual challenges. In one track, a power glitch during precalibrations kept the operators busy recooling the Ka-band HEMT to bring it back online as quickly as possible. In another, the first local oscillator lost lock with the frequency reference and ran noncoherently with the rest of the station. On one occasion, because of a receiver problem, the operator at DSS 13 had to perform manual boresights of the antenna using carrier estimates from a Pioneer-10 receiver located at SPC-10.

Eventually, through much perseverance on the part of station personnel and subsystem engineers, the system irregularities and interface problems were eliminated. Towards the end of KaBLE, operations took on a more routine nature, and preparations were underway to handle the more operationally challenging mapping phase of the Mars Observer mission when Doppler dynamics would increase a hundredfold and carrier reacquisitions would occur about eight or nine times per track.

VI. Experiment Results

As discussed earlier, KaBLE was divided into three tasks: a telemetry demonstration, a ranging demonstration, and a tracking experiment. The goal of the telemetry demonstration was to prove the feasibility of a telemetry link at Ka-band by collecting a minimum of 1 million bits of quality 250-bit/sec data. The goal of the ranging experiment was to perform a similar demonstration of Ka-band ranging. The goal of the tracking experiment was to develop a database of Ka-band link statistics, including weather, noise temperature, and antenna performance, for use in the development of future missions and ground stations at Ka-band. For the most part, all three goals were achieved by KaBLE. Both telemetry and ranging demonstrations were successful. However, because of the untimely end of Mars Observer, the tracking experiment was able to acquire only a partial database of antenna performance. The results of the three phases of KaBLE and a preliminary analysis are discussed below. Further study of Ka-band antenna performance is covered in the next section.

A. Telemetry Demonstration

A certain amount of difficulty is normally expected whenever a new technology is demonstrated, so it is not surprising that a number of obstacles arose during the KaBLE telemetry demonstration. The first obstacle was the weather. By an unfortunate coincidence, the telemetry demonstration took place during one of the worst weather systems to ever hit the Goldstone area. Heavy rains, flashfloods, and dense fog were daily occurrences. During one track, a blanket of wet snow covered the antenna and ground.

This type of weather has a major impact on Ka-band performance, since the Ka-band is adjacent to the water absorption lines in the RF spectrum. Noise temperature at Ka-band seldom dropped below 90 K during these 2 weeks, and sometimes, at low elevations, reached as high as 250 K. This, in itself, should not eliminate the use of Ka-band in the DSN, since weather of this nature is so rare (99.9-percent probability of not occurring compared to the 90-percent weather tolerance allocated in the KaBLE link budget). However, for the duration of the telemetry demonstration, weather was a major limiting factor in data collection.

Given the extreme weather conditions, the use of a beam-waveguide antenna for KaBLE proved to be a wise choice. Even though the dish was saturated most of the time, the Ka-band front-end, in particular the feedhorn

cover, was kept dry in the shelter of the pedestal room. Had an extra layer of water been allowed to collect on the feedhorn cover, as would be the case in a Cassegrain feed antenna, the telemetry demonstration would have collected even less data at Ka-band, perhaps none.

A second obstacle involved the spacecraft. Due to an anomaly in the Attitude Control Subsystem (ACS), Mars Observer delayed switching on the HGA (and hence the Ka-band downlink) until 3 days into the 14-day telemetry demonstration. Furthermore, once the HGA was turned on, an antenna calibration maneuver revealed a large (1.1-deg) pointing error. This resulted in an unplanned loss of signal level—about 6.7 dB at X-band and 3.5 dB at Ka-band as derived in Section VI, which the spacecraft team could not correct until after orbit insertion.

On the first night of tracking, a final obstacle was encountered: a polarization mismatch resulting in a 10- to 15-dB loss in signal level at Ka-band. It took several days of testing to recognize the problem and isolate the source. The tests that were performed included injecting right- and left-hand circularly polarized (RCP and LCP) signals into the KaBLE ULNA, switching to the backup Ka-band HEMT, and inserting a half-wave plate into the signal path while tracking to reverse the polarization of the downlink signal. The last test proved the most conclusive, resulting in about 10 dB of signal gain with the half-wave plate installed. But to achieve the desired minimum noise temperature, a more permanent solution was needed. With only 4 days remaining before the end of the demonstration, the ULNA was warmed, reconfigured to the correct RCP polarization, and brought back on line, all within a 36-hr period. Again, easy access to the Ka-band front-end provided by the layout of a beam-waveguide antenna proved critical to the eventual success of the demonstration.

While the polarization problem was being corrected, meetings were held at JPL with the Mars Observer team to incorporate "on-the-fly" KaBLE input into the configuration of the spacecraft. Because of the weather and the increased spacecraft pointing loss, the signal hovered very near the 250-bit/sec threshold. A plan was implemented to allow the KaBLE principal investigator to decide, based on the weather forecast at 4 p.m., whether to proceed with a 250-bit/sec track or a reduced 10-bit/sec track (for higher signal margin). A phone call to the spacecraft team at 4 p.m. would result in a change in spacecraft configuration 2 hr later; this change would then have to remain constant for the duration of the track.

During the remaining 3 days, the weather continued wet and cold, but the 250-bit/sec configuration was chosen for all 3 days. On the first day, the signal never cleared the 250-bit/sec threshold. On the second day, station personnel pulled the dichroic plate in the hope that some data might clear the threshold because of the reduced Ka-band noise temperature, even though no real-time confirmation of Ka-band data quality would be possible without X-band data. Shortly after the dichroic plate was reinstalled, the weather eased and the first burst of good data was collected. In spite of 3 dB of extra spacecraft pointing loss and persistently bad weather, a total of 3 hr of good data (about 3 million bits) was collected on that day. On the last day, the signal remained below the 250-bit/sec threshold for the duration of the track.

A plot of tracking statistics for the successful telemetry track is shown in Fig. 9. The carrier-to-noise ratio (P_c/N_0), SNT, and antenna elevation are shown in comparison with the received bit-error rate. The gap in X-band SNT covers the period when the dichroic plate was removed. The first burst of good data, which came after the plate was reinstalled, lasted only about 6 min, at which point the spacecraft changed mode from three-way operation with DSS 65 uplinking to one-way operation; the weather worsened, and antenna efficiency dropped as the elevation approached 70 deg. It was not until the weather eased and the elevation neared the rigging angle (50 deg) that the data improved again, this time for 3 hr. The bit-error rate ranged from 50 percent (or -3 on the log scale) at the start of the track to about 1 percent (or -20) during peak performance, which is adequate proof of the successful acquisition of Ka-band telemetry data.

B. Ranging Demonstration

Work on the KaBLE ranging demonstration began shortly after the telemetry demonstration ended. The goal of this effort was to demonstrate the demodulation of DSN ranging codes at Ka-band. Also, it was hoped that the X-/Ka-band differential range could provide a new data type for radio-science observations near solar conjunction (a hope that was not realized due to the loss of Mars Observer).

A dual-channel ranging system for KaBLE was obtained at virtually no extra cost to the experiment by sending the IF signals from DSS 13 over the existing optical-fiber link to the ranging equipment at SPC-10. The SPC-10 equipment included two Pioneer-10 (P10) receivers, which are prototypes for the Block-V receiver, and a modified sequential ranging assembly (MSRA), a standard SRA modified to interface with the P10 receivers.

Figure 10 shows the ranging system configuration for KaBLE. The heavy lines represent the ranging signal path

for the demonstration. While DSS 15 performed normal two-way ranging with Mars Observer at X-band, the P10/MSRA assembly performed three-way ranging using the X- and Ka-band signals received at DSS 13. Ranging data were logged on a personal computer, which interfaced with the MSRA through a maintenance port.

Two successful ranging passes were obtained for KaBLE. On day of year (DOY) 56, 32 valid range points were collected, while on DOY 76, a total of 60 points were collected, 14 of which were discarded due to antenna mispointing. The ranging modulation was identical for both passes: a 20-sec integration time for the clock component (1 MHz) followed by 10 sec at each of the seventeen successive components for a total cycle time of 3 min and 30 sec per range point. Analysis of the data from these two passes, summarized below, indicates good agreement between the measured ranging signal-to-noise ratio (SNR) and the accuracy of the range estimates.

The ranging SNR (P_r/N_0) for the two passes is shown in Fig. 11. Because the modulation index is four times higher at Ka-band, the difference in X- and Ka-band ranging SNR is only about 20 dB (compared to the 35-dB difference in carrier power). Nevertheless, on DOY 76 the increased fluctuation in P_r/N_0 estimates indicates that the code strength neared threshold for the measurement integration time.

Figure 12 shows the X-/Ka-band differential range for the two passes measured in range units (RU) of the round-trip light time (1 $RU \approx 0.952$ nsec). The bias in the data on the first chart (DOY 56) shows that the Ka-band path was 26 RU longer than the X-band path, which is consistent with the layout of the DSS-13 system. The bias in the second chart shows that the offset increased to 67 RU on DOY 76, which is also consistent with a cable bypass in the X-band path on that day.

The range residuals for each channel are shown in Fig. 13. The residuals are relative to a sixth-order curve fit made on the X-band data. The difference in delays measured for the X- and Ka-band paths can again be identified by the 26-RU and 67-RU offsets between the two curves. The standard deviation of the residuals is listed in Table 5 and compared with the expected standard deviation based on the average ranging SNR (P_r/N_0) measured during the pass. At X-band, the measured sigma is about twice the expected sigma, which may be due to errors in the model used to form the prediction. At Ka-band, there is close agreement between the average P_r/N_0 and the measured sigma, although on DOY 76 the measurement is slightly better than expected. This is probably due to the large fluctuations in P_r/N_0 during that pass.

C. Tracking Experiment

The tracking experiment covered the period from deployment of the Mars Observer HGA in January 1993 to just prior to the Mars Orbit Insertion in August. During this 9-month period, 27 tracks were performed for a total of 291 hr. However, due to the large number of problems that occurred while tracking, only about 164 hr of Ka-band tracking data were obtained.

During the 9 months of the tracking experiment, the KaBLE system underwent frequent changes as new equipment was installed and subsystems were upgraded. The Ka-band maser was removed a few weeks after the telemetry demonstration and the Ka-band HEMT—with higher noise temperature but lower maintenance costs—was installed in its place. The TP-13 Advanced Receiver was swapped in and out to support experiments with the Galileo spacecraft. The Antenna Monitor and Control subsystem was improved with hardware and software upgrades to allow boresighting from the control room and faster response time. Through it all, a viable KaBLE configuration was maintained.

Table 6 summarizes the results of each track. In general, the problems that occurred were due mainly to subsystem failures or interfacing problems, and so the shortfall in data collection does not reflect any limitations in the performance of a Ka-band downlink. As discussed in Section V, the problems that arose during KaBLE tracks were quite varied and numerous. In fact, experience gained with these problems was a valuable by-product of KaBLE and will go a long way toward improving the design and implementation of a Ka-band tracking subnet in the DSN.

On some occasions, KaBLE tracks were limited by a combination of bad weather and poor signal strength. For instance, almost all of the tracks during the telemetry demonstration (DOYs 8 through 17) were affected by the heavy rains. Also, on DOYs 76 and 95, the wind was so high (and the carrier signal so low) that proper tracking was impaired. (On DOY 95 the antenna had to be stowed for several hours until the winds died down.) As an example of the data set collected by KaBLE, tracking results for three separate tracks—DOYs 18, 56, and 197—are shown below.

1. DOY 18. This track, which followed the last day of the telemetry demonstration, was performed with the spacecraft configured for carrier only at Ka-band (i.e., no telemetry). Also, the spacecraft transponder was referenced to the DSS-15 uplink. At the time, a problem with the DSS-15 exciter led to cycle slips in the X- and Ka-band downlinks whenever DSS 15 was uplinking. These cycle

slips, which show very clearly in Fig. 14 as 10- to 20-dB dropouts in received carrier power, tended to interfere with efforts to boresight the DSS-13 antenna. Consequently, much of the track was performed in a blind-pointing mode. The descending arc from hour 27 to 31 represents the accumulation of pointing errors in the blind-pointing model until the boresight at hour 31 corrected the pointing error.

The weather and noise temperature statistics for this track are shown in Fig. 15. On this day, the weather was similar to that during much of the telemetry demonstration in that a layer of heavy clouds rolled in shortly after the track began, bringing fog and rain with them. The weather signature can be seen clearly in the Ka-band system-noise-temperature curve.

2. DOY 56. DOY 56 was the day of the first successful Ka-band ranging demonstration. The tracking results in Figs. 16 and 17 complement the ranging data presented in Part B of this section. As in DOY 18, only a few boresights were performed, so as not to interfere with the ranging measurement. The scalloped signature of the Ka-band received carrier power in Fig. 16 is essentially due to the blind pointing error of the DSS-13 antenna.

The weather for the track was clear with only a thin, high-altitude haze. Humidity is seen to be rising throughout the track, but its effect on carrier power is negligible. The Ka-band noise temperature is about 70 K, due to the higher noise Ka-band HEMT that was installed in place of the ULNA.

3. DOY 197. This track came at the end of a difficult week of tracking. The intention was to obtain a large quantity of high-quality data during one week to make up for a 2-month hiatus in tracking over the summer. To this end, system health was verified during a track on DOY 172, and the Ka-band maser was reinstalled to obtain optimum noise-temperature performance.

During the first day of this week, DOY 193, problems arose with a gateway that had been installed to buffer the AMC from LAN traffic. Efforts to debug the problem took up the next 3 days, during which the antenna could not be boresighted. On the second day, the maser began to experience some difficulties, including a higher than normal system noise temperature (60 to 80 K) and recurring gain fluctuations, the source of which is under investigation. But on Friday, DOY 197, the system temperature returned to about 41 K and the AMC gateway problem was corrected.

Figure 18 shows the tracking data from the DOY 197 track. Minicalibrations of system noise temperature and antenna boresights were performed on the hour, as indicated by the downward spikes in received carrier power. Note that even with the maser, the Ka-band carrier-to-noise ratio was only about 10 dB-Hz, since the spacecraft at this time was approaching opposition. The low signal level results in about 2 to 3 dB of spread in carrier-to-noise ratio estimates.

In Fig. 19, the weather and noise temperature statistics are shown. Here the hourly minicalibrations show as vertical lines in the system noise temperature curves. The remnants of the Ka-band maser gain fluctuations can be seen in the 2- to 3-K difference in noise temperature before and after each minicalibration. The most accurate SNT measurements are those following the minicalibrations. In terms of weather, the track was performed under nearly ideal conditions: clear skies, low humidity, and light winds.

D. Preliminary Analysis of Tracking Data

The basic goal posed at the outset of KaBLE was to determine how Ka-band ranks in comparison to X-band for use in deep-space communications. The question is complex, since there are many different ways of evaluating a communications link. This section reviews some of the analysis that has been performed to place the KaBLE results in a suitable context for further comparisons with X-band.

1. Spacecraft Pointing Loss. The first analysis for KaBLE involved the determination of the spacecraft pointing loss, a critical factor needed for further analyses. Pointing losses were estimated using DSN tracking data during the HGA calibration maneuver on DOY 8. During the maneuver, the spacecraft was offset 0.5 deg from the Earth line and allowed to rotate one full turn (lasting 100 min) while the uplink and downlink signals were observed. Had the HGA been properly pointed along the Y-axis there would be no significant variation in signal level other than an initial step of about -1 dB when the 0.5-deg offset was inserted.

However, what was actually observed in the tracking data from DSS 65 was a sinusoidal signature in carrier power with an amplitude variation of about 15.3 dB. This observation provides an accurate means of determining pointing offset. Figure 20 shows the Mars Observer HGA gain at X- and Ka-bands along with the variation in X-band power that would be observed during the maneuver, assuming a given pointing error. Note that the Ka-band beam pattern is actually wider than X-band because of the smaller Ka-band antenna. Based on this chart, the

measured variation of 15.3 dB implies a pointing offset of 1.1 deg, or a pointing loss of 6.7 dB at X-band and 3.5 dB at Ka-band. This derivation agrees well with similar data on measured uplink variations during the maneuver, and is accurate to about 0.2 dB or less.

2. Comparisons With Theory. One way to gain understanding of the Ka-band downlink, in light of the unanticipated spacecraft pointing losses, is to use measurements of signal level from a KaBLE track to estimate the spacecraft EIRP. This is done in Table 7 for the track on DOY 197. The procedure for deriving EIRP is to work backwards through the link budget, starting with measurements of P_c/N_0 and adjusting for the effect of each parameter. Both P_c/N_0 and system noise temperature were sampled at 50 deg elevation, the rigging angle of the DSS-13 antenna, and inserted into the table along with the pointing-loss estimates derived above, modulation loss estimates (due to ranging and telemetry modulations) obtained from laboratory data,[9] and the rest of the link budget parameters.

The resulting EIRP estimates come very close to those derived in the link budget of Table 3. The X-band estimate is 0.3 dB higher than theory, while the Ka-band estimate is about 1 dB higher. Although somewhat higher than planned, the Ka-band value does fall within the tolerance of the link budget estimate and may explain why the telemetry demonstration was successful in spite of the extra pointing loss. The uncertainty in this estimate is about 1.2 dB at Ka-band (0.4 at X-band) and can be reduced by sampling data from other tracks.

A similar analysis was used to derive the plot in Fig. 21. Here a theoretical estimate of total signal-to-noise ratio (P_t/N_0) versus time was derived from the link budget by varying the antenna G/T as a function of elevation angle. Then the theoretical curve was overlaid upon the actual tracking data, in this case the track on DOY 17 for 0- and 90-percent weather conditions. The result shows a strong correlation between measured P_t/N_0 and theory, with the actual signal appearing about 1 dB below the 90-percent line. At either end of the curve, the measurement falls farther away from theory, which may be due to deterioration of the weather. (See Fig. 9 for more DOY 17 tracking statistics.)

3. Link Normalization. Because of the difference in X- and Ka-band radiated power from the Mars Observer spacecraft, there is a large difference in received carrier power at X- and Ka-bands. One of the first steps toward obtaining a fair comparison is to normalize the two downlinks. This requires the development of correction factors for both ends of the link: the spacecraft and the receiver.

Spacecraft normalization is derived in Tables 8 and 9. Column 2 of Table 8 shows the EIRP budget for the Mars Observer X-band transmitter. Column 3 develops the estimated EIRP for a normalized Ka-band transmitter: in other words, a Ka-band beacon that transmits the same power through the same-sized antenna as X-band. Comparisons to the actual KaBLE beacon can be made with the numbers in column 4.

Several important assumptions have been made in normalizing the Ka-band transmitter. The first and most important is that the power amplifier efficiency on board the spacecraft is the same at X- and Ka-bands. Although current technology does not support this assumption, new developments in power amplifier design are making frequency less of an issue. The second is that antenna efficiency and pointing losses will be the same at both frequencies. All of the assumptions depend upon spacecraft design, and so cannot be considered exact. The point of this exercise is to offer a reasonably fair comparison for the sake of understanding relative link performance.

Table 9 derives the overall spacecraft correction factor by combining the change in EIRP with spacecraft pointing and telemetry losses. The pointing loss was calculated in section VI.D.2. The modulation losses, both ranging and telemetry, were derived from measurements of the actual flight unit in the laboratory.

The normalization of the receiver is simpler than the spacecraft, consisting only of a noise temperature correction for obtaining a common reference: the best possible performance at DSS 13. For Ka-band, this requires removing the dichroic plate and optimizing the beam waveguide. For X-band, this requires switching to a ULNA. These correction terms are shown in Table 10.

Figure 22 shows the results of applying the correction factors to the tracking data from DOYs 18, 56, and 197. In spite of the wide scatter in Ka-band power estimates (due to the very low SNR) the potential improvement of Ka-band can be seen to range from 4 to 7 dB. Also, the relative advantage on a day like DOY 18, which was cloudy and wet, is seen to be about 1 dB less (disregarding ground station pointing errors) than a day like DOY 197, which was clear and calm.

[9] J. F. Weese, "Third Week Report for the Mars Observer Flight Panel Testing Accomplished in the Telecommunications Laboratory (TDL) from 4/29/91 through 5/3/91," Interoffice Memorandum 3395-91-054 (internal document), Jet Propulsion Laboratory, Pasadena, California, October 10, 1991.

From here, the analysis can be taken still further, for instance by integrating the performance difference over an entire track. This would provide a single measurement of the Ka-band performance improvement for the track, including the effects of pointing errors and weather degradations while smoothing the effects of measurement scatter. Other goals for KaBLE data analysis include the development of a model of Ka-band link degradation as a function of weather and a study of the DSS-13 antenna performance. These goals will be carried out by the successor project to KaBLE, the Ka-Band Antenna Performance (KaAP) Experiment.

VII. Future Work

KaBLE ended due to the loss of communications with the Mars Observer spacecraft on August 21, 1993. However, the primary goal of KaBLE, characterizing Ka-band link performance, was far from complete. Compilation of accurate statistical weather models and ground-antenna performance parameters require much more data than that obtained during the 8 months of the experiment. To continue the work begun by KaBLE, a new experiment, the Ka-band antenna performance study was begun. The objective of the KaAP study is to characterize the antenna performance of DSS 13—its efficiency, G/T, pointing accuracy, and weather sensitivity—using quasars and other natural radio sources at X- and Ka-bands. In addition, studies and proposals are under way to equip future deep-space and Earth-orbiting spacecraft with Ka-band transmitters to conduct follow-on experiments with coherent signals.

Other plans for Ka-band include the Cassini Mission to Saturn, which will conduct radio science experiments at X- and Ka-bands, and the Gravitational Wave Experiment planned for the late 1990's, which will utilize dual X- and Ka-band signals coherent with a ground-to-spacecraft uplink. At that time, Ka-band radio links in deep space would become an operational aspect of the DSN.

The data analysis presented in this article is preliminary. Work will continue to further process and analyze KaBLE's data set to improve on the statistical aspect of the results.

Acknowledgments

Many people from JPL and Astro contributed to the success of this experiment—more than can fit on this one brief list. On the spacecraft side, thanks to Lance Riley and Dan Rascoe of JPL for initiating the Ka-band beacon with Astro; Bob Ostovarpoor of Astro for doubling the power of the beacon; Jim Weese of JPL for flight and ground compatibility testing at JPL, Astro, and Cape Canaveral; Jack Meeker, John Koukos, and Victor Lo for analysis and planning; and the Mars Observer Flight Project—especially Glenn Cunningham, Charles Whetsel, and Suzanne Dodd—for accommodating the needs of the experiment.

On the ground side, we thank Mark Gatti for overseeing the DSS-13 implementation; George Rinker for predicts generation; Farzin Manshadi for the dichroic plate; Leon Alvarez, Caroline Racho, and Martha Berg for antenna pointing; Jim Shell, Gary Glass, and Mark Fiore for the Ka-band maser; Bob Clauss for clinching the polarization problem; Eric Paulsen and Loris Robinett for receiver and Doppler tuner development; Ramin Sadr, Roland Bevan, Remi La Belle, and Robert Lee for the advanced receivers and data handling terminal; Sumita Nandi for tone tracker support; and Randy Heuser and Richard Chen for the monitor and control subsystem. The ranging demonstration could not have been performed without the spare Pioneer-10 receiver provided by Jack Childs and Jeff Berner, the new fiber-optic transceivers provided by George Lutes, and the ranging interface modifications made by Hal Baugh and Miguel Marina.

The authors particularly thank Lyle Skjerve and the staff of DSS 13, especially Gary Bury, Jerry Crook, Ron Littlefair, and Juan Garnica, for excellent service and

for finding various ways to improve the design and operation of the KaBLE ground system.

Finally, we thank Sami Asmar and Trish Priest for help in the preparation of this article, and David Morabito for his meticulous review.

References

[1] J. G. Smith, "Ka-Band (32-GHz) Downlink Capability for Deep Space Communications," *The Telecommunications and Data Acquisition Progress Report 42-88, vol. October–December 1986*, Jet Propulsion Laboratory, Pasadena, California, pp. 96–103, February 15, 1987.

[2] J. W. Layland and J. G. Smith, "A Growth Path for Deep Space Communications," *The Telecommunications and Data Acquisition Progress Report 42-88, vol. October–December 1986*, Jet Propulsion Laboratory, Pasadena, California, pp. 120–125, February 15, 1987.

[3] A. L. Riley, D. M. Hanson, A. Mileant, and R. W. Hartop, "A Ka-band Beacon Link Experiment (KABLE) With Mars Observer," *The Telecommunications and Data Acquisition Progress Report 42-88, vol. October–December 1986*, Jet Propulsion Laboratory, Pasadena, California, pp. 141–147, February 15, 1987.

[4] J. Shell and R. B. Quinn, "A Dual-Cavity Ruby Maser for the Ka-Band Link Experiment," *The Telecommunications and Data Acquisition Progress Report 42-116, vol. October–December 1993*, Jet Propulsion Laboratory, Pasadena, California, pp. 53–70, February 15, 1994.

[5] W. H. Press, B. P. Flannery, S. A. Teukolsky and W. T. Vetterling, *Numerical Recipes*, New York: Cambridge University Press, pp. 147–151, 1989.

Table 1. Mars Observer Spacecraft EIRP derivation for X- and Ka-band.

Parameter	X-band	Ka-band
Antenna diameter, m	1.5	0.28
1-dB beamwidth	0.9	1.3
Beam alignment, dB	0 (Ref.)	<0.1
EIRP budget		
Power, dBm	46.5	15.3
Circuit loss, dB	−3.4	−0.8
Antenna gain, dBi	39.8	37.0
Pointing loss, dB	−0.9	−0.5
Total *EIRP*, dBmi	82.0	51.0

Table 2. Ka-band G/T budget for DSS 13 at the rigging angle (50 deg el), assuming 90-percent weather conditions.

Parameter	Gain, dB	Physical temperature, K	Effective temperature, K
Maser and follow-on	0.0 (Ref.)	5.2	5.2
Cooled horn and waveguide	−0.27	1.8	1.8
Dichroic plate	−0.11	7.5	7.0
Antenna at F3 (at 50 deg el)	78.28	15.6	14.3
Atmosphere (90 percent at 50 deg el)	−0.28	17.9	16.4
Cosmic background	0.00	2.0	1.7
Subtotal	77.62	—	46.4
	−16.66		(16.66 dBK)
G/T	60.95		

Table 3. KaBLE link budget at end of telemetry window, January 18, 1993.

Parameter	X-band	Ka-band
Spacecraft $EIRP$, dBmi	82.0	51.0 ± 1
Space loss (0.37 AU), dB	−267.8	−277.9
DSS-13 G/T (above 30 deg el), dB	54.1	60.5 ± 0.7
DSS-13 pointing and polarization loss, dB	−0.1	−0.6 ± 0.4
Boltzmann's constant, dBm-K-Hz	198.6	198.6
P_t/N_0, dB-Hz	66.8	31.6
Telemetry modulation loss (59.9 deg), dB	−1.3	−1.5 ± 0.2
Processing loss, dB	−0.3	−1.0 ± 0.5
Data rate (250 bits/sec), dB-Hz	−24.0	−24.0
Decoder threshold, dB	−3.0	−3.0
Link margin, dB	38.2	2.1 ± 1.4

Table 4. DSS-13 technical requirements for KaBLE.

Item	Requirement
Antenna pointing error, mdeg rms	< 2.0
Microwave band, GHz	33.66 to 33.7
System noise temperature, K	33 ± 2 (90-percent weather)
Telemetry data rate, bits/sec	250
Ranging capability	Functional
Data acquisition	Various tracking statistics

Table 5. Standard deviation of ranging measurements at X- and Ka-band compared with expectation from average P_r/N_0.

Track		Average P_r/N_0, dB-Hz	Expected sigma, RU	Measured sigma, RU
DOY 56	X-band	24.3	1.9	4.3
	Ka-band	3.4	21.2	25.1
DOY 76	X-band	20.9	2.8	4.6
	Ka-band	−1.6	37.7	34.4

Table 6. Summary of KaBLE tracking results.

DOY, 1993	Track, hr	Ka-data, hr	Weather	Remarks
8	12	8	Clouds and rain	Polarization mismatch
9	12	1	Clouds and rain	Polarization mismatch
10	12	10	Clouds, wind, and rain	Polarization mismatch
11	12	10	Clouds and rain	Polarization mismatch
12	12	1	Clouds, rain, and snow	Polarization testing
13	12	2	Clouds and rain	Decision to reconfigure maser
14	12	3	Heavy clouds and rain	Ka-band HEMT
15	12	6	Heavy clouds and rain	Maser back on line
16	12	11	Scattered clouds, rain	Telemetry demonstration success
17	12	10	Clouds and rain	Cannot clear TLM threshold
18	12	10	Clouds and rain	Carrier tracking only
28	8	4	Clear	Receiver problem
35	8	0	Clear	First LO free running
42	8	4	Clear	Ka–HEMT glitch (warm)
49	8	1	Clouds and rain	Power out–receiver crash
56	8	6	Clear	Ranging demonstration success
76	8	3	Clear and windy	Range data, interface problem
89	8	6	Clear and windy	DHT problem
95	8	3	High winds	Antenna wind limit (stow)
96	9	8	Clear	Interface problems
172	8	4	Clear	DHT problem
193	5	2	Clear	AMC problem
194	9	4	Clear	AMC/maser problems
195	10	8	Clear	AMC/maser problems
196	10	6	Clear	Maser G/T instability
197	10	10	Clear	AMC ok, maser stable
207	10	6	Clear	DHT problem
211	10	9	Clear	Ka–HEMT (low SNR)
217	7	4	Clear	LO tuning

Table 7. Derivation of KaBLE EIRP from DOY 197 tracking data shown with predicted EIRP from Table 1.[a]

Parameter	X-band	Ka-band
Measured P_c/N_0 (at 50 deg el), dB-Hz	**43 ± 0.2**	**11 ± 1**
Modulation losses, dB	3.3 ±0.2	4.1 ± 0.2
Boltzmann's constant, dBm-K-Hz	−198.6	−198.6
Polarization and circuit loss, dB	0	0.2
Measured SNT, dBK	**15.4 ± 0.1**	**16.4 ± 0.2**
DSS-13 pointing loss, dB	0.1	0.5 ± 0.2
DSS-13 gain (at 50 deg el), dB	−68.11 ± 0.1	−77.9 ± 0.5
Atmospheric attenuation, dB	0	0.3
Space loss, dB	280.5	292.5
Spacecraft pointing loss, dB	6.7 ± 0.2	3.5 ± 0.2
Estimated *EIRP*, dBmi	82.3 ±0.4	52.0 ± 1.2
Predicted *EIRP*, dBmi	82.0	51.0

[a] Tracking data are in boldface.

Table 8. Normalized Ka-band EIRP budget for performing X- and Ka-band link comparisons, assuming the same power amplifier efficiency, circuit loss, antenna diameter (and efficiency), and pointing loss as that for X-band.

Parameter	X-band	Normalized Ka-band	KaBLE
Dish diameter, m	1.5	1.5	0.28
Power, dBm	46.5	46.5	15.3
Circuit loss, dB	−3.4	−3.4	−0.8
Antenna gain, dBi	39.8	51.8	37.0
Pointing loss, dB	−0.9	−0.9	−0.5
Totals			
EIRP, dBmi	82.0	94	52 (DOY 197
$\Delta EIRP$ (normalized KaBLE)	0.0	42	estimate)

Table 9. Correction factor for converting measured X- and Ka-band carrier SNR (P_c/N_0) into a comparative total SNR (P_t/N_0) based on EIRP normalization in Table 8, spacecraft pointing loss estimated in Section VI.D.1., and modulation losses from laboratory measurement.

Parameter	X-band	Ka-band
$\Delta EIRP$, dBmi	0.0	42
S/C pointing loss (estimate), dB	6.7	3.5
Modulation loss (ranging + TLM), dB	3.3	4.1
Correction factor, dB	10.0	49.6

Table 10. Receiver system noise temperature corrections to obtain common reference point, i.e., best possible SNT obtainable at DSS 13 for performing link comparisons.

Band	Best possible DSS-13 SNT	Actual		Correction	
		SNT_{ULNA}	SNT_{HEMT}	ΔT_{ULNA}	ΔT_{HEMT}
X	18	18	33	0	15
Ka	25	41	65	16	40

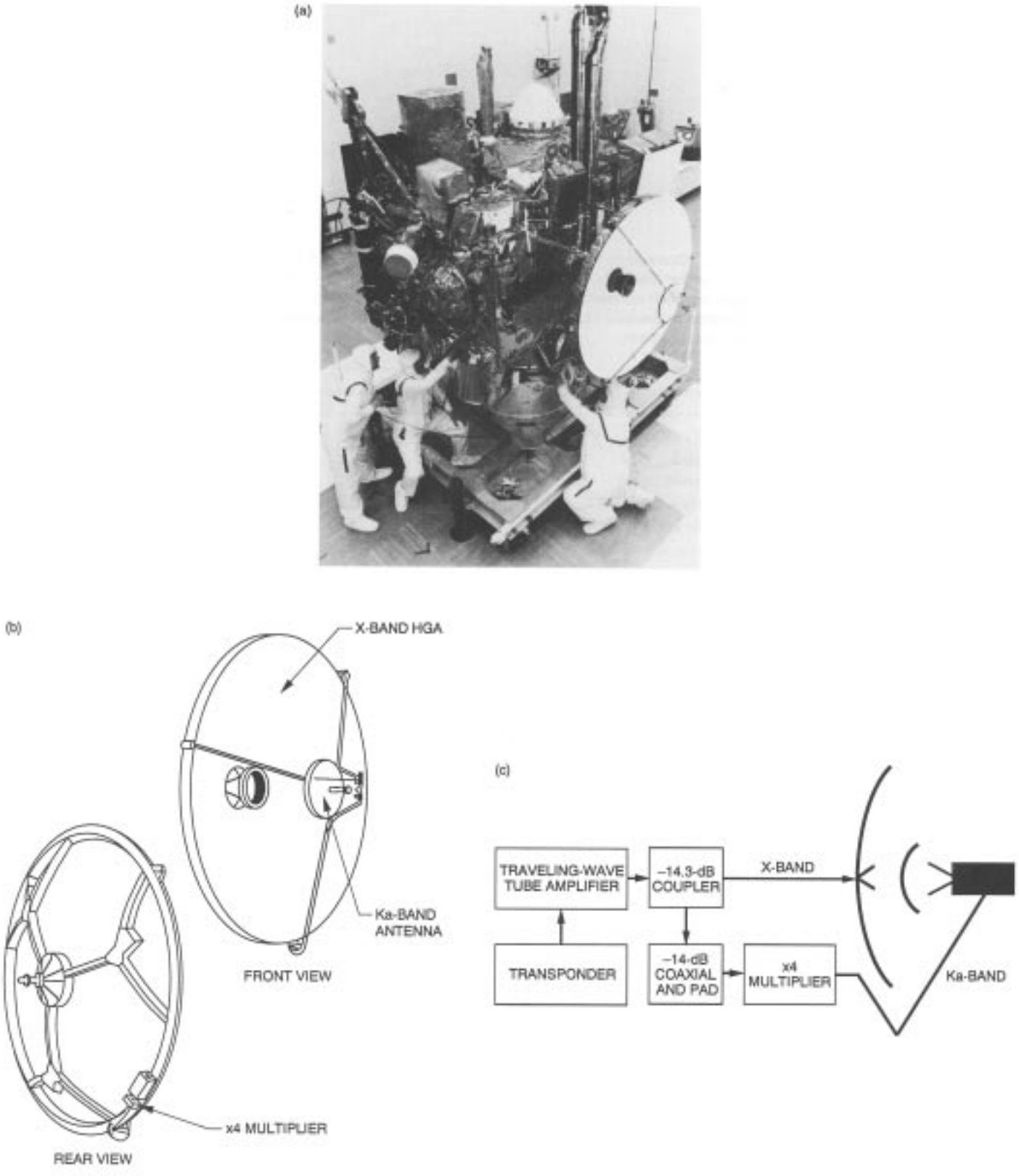

Fig. 1. KaBLE equipment on the Mars Observer spacecraft: (a) the spacecraft during preflight inspection; (b) HGA showing Ka-band antenna and times-four multiplier; and (c) transponder RF components.

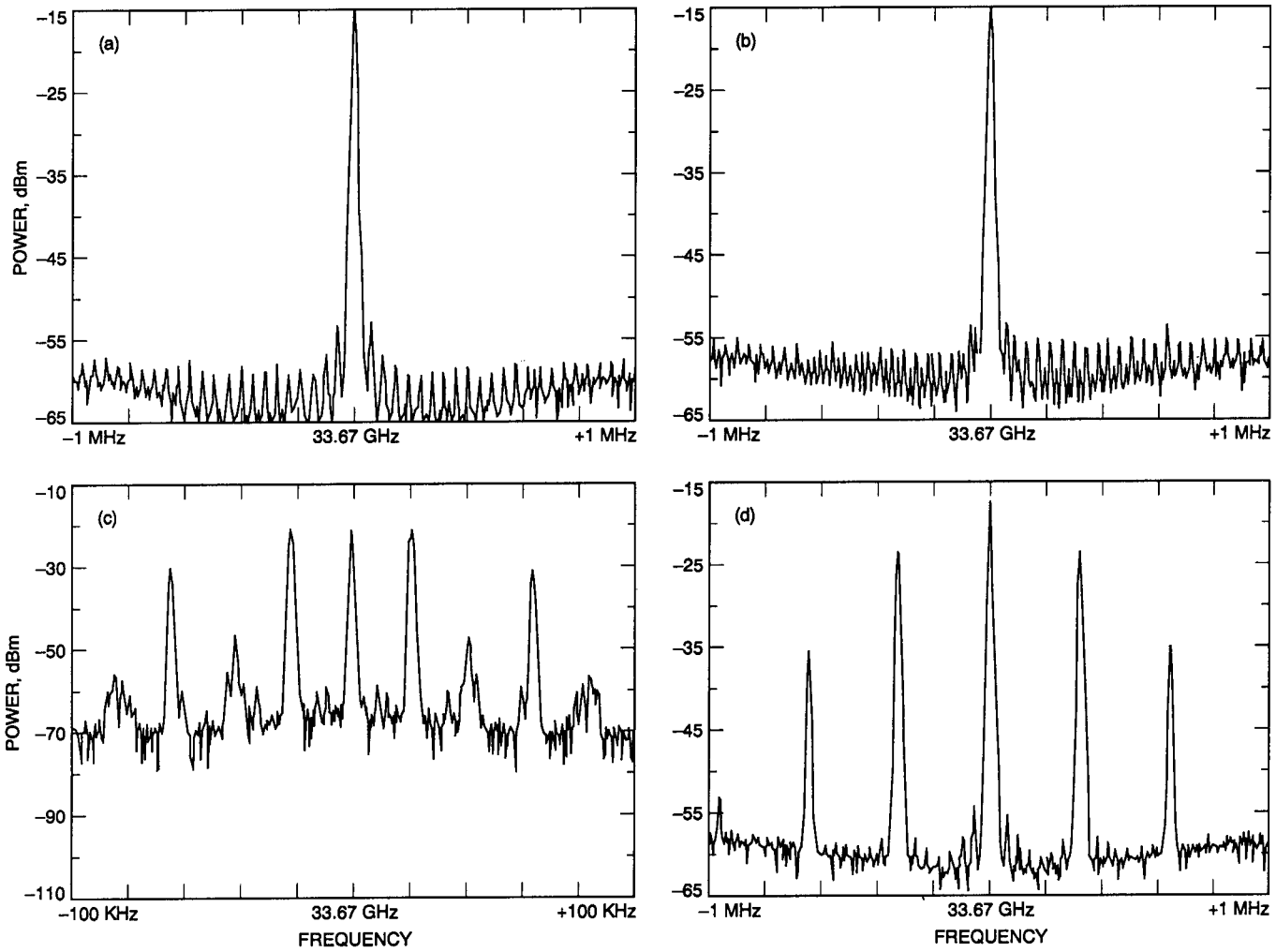

Fig. 2. Ka-band spectra from Mars Observer electromagnetic emissions test, showing the Ka-band carrier supression for X-band modulation indices of (a) 0 deg, (b) 44.8 deg (used for tracking experiment), (c) 59.9 deg (used for telemetry demonstration), and (d) 80 deg (used for mapping orbit tracking).

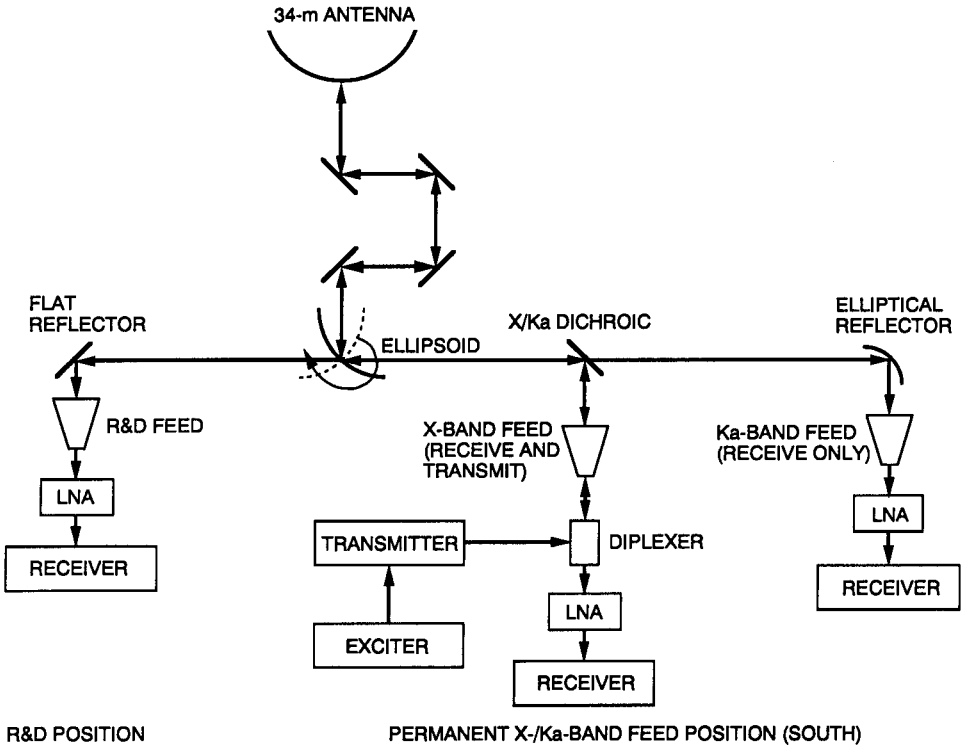

Fig. 3. DSS-13 microwave subsystem with the components included in the *G/T* budget of Table 2.

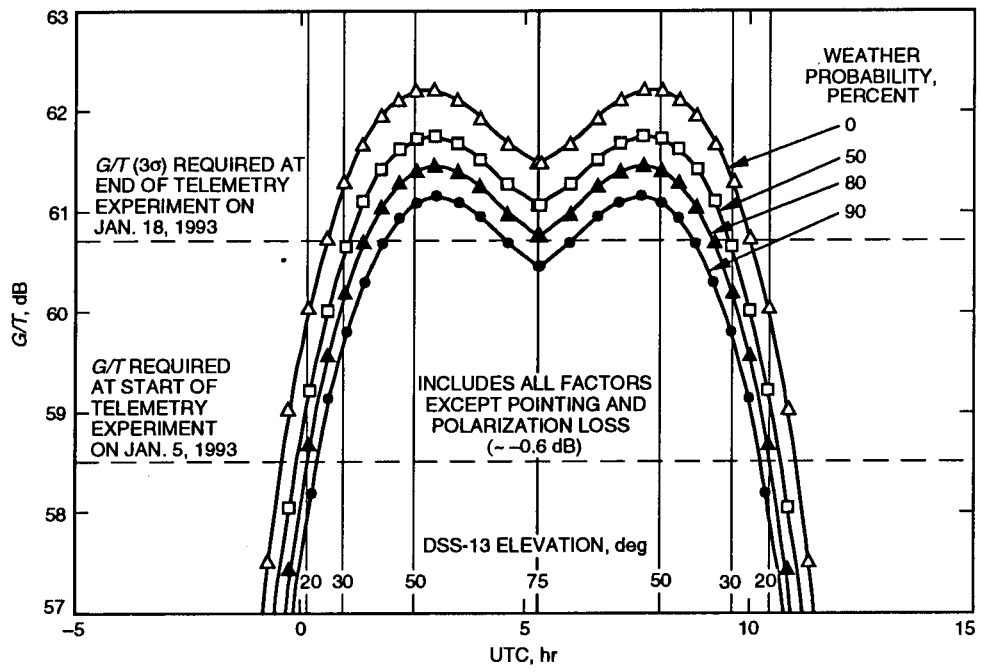

Fig. 4. DSS-13 *G/T* at 33.7 GHz versus time for a track in January 1993, showing the minimum requirements for telemetry reception and the effects of various weather conditions.

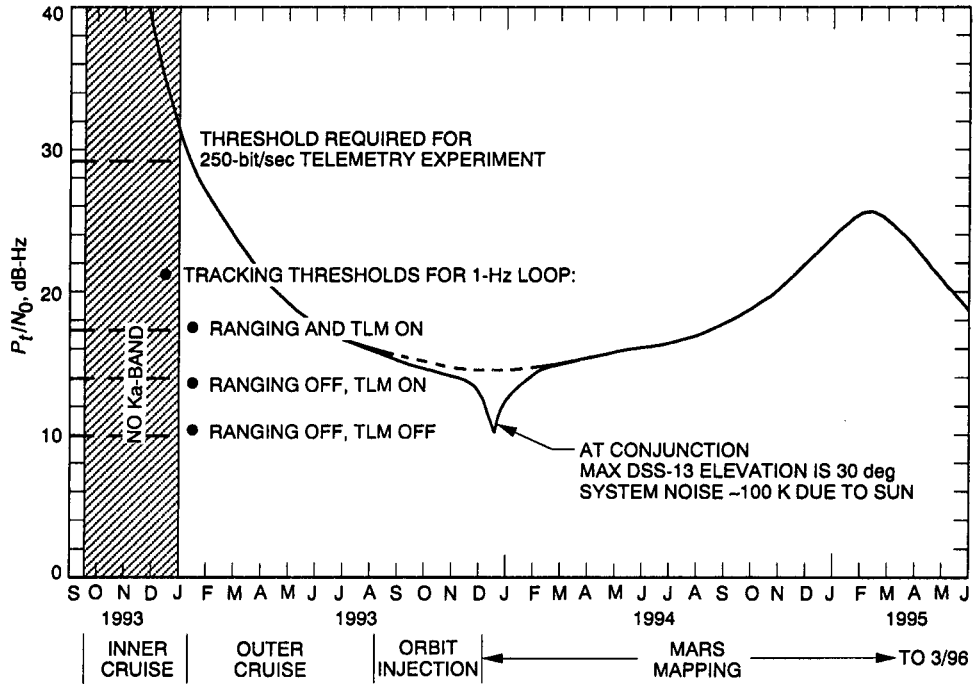

Fig. 5. Received Ka-band signal strength at DSS 13 expected over 2 years of the KaBLE experiment.

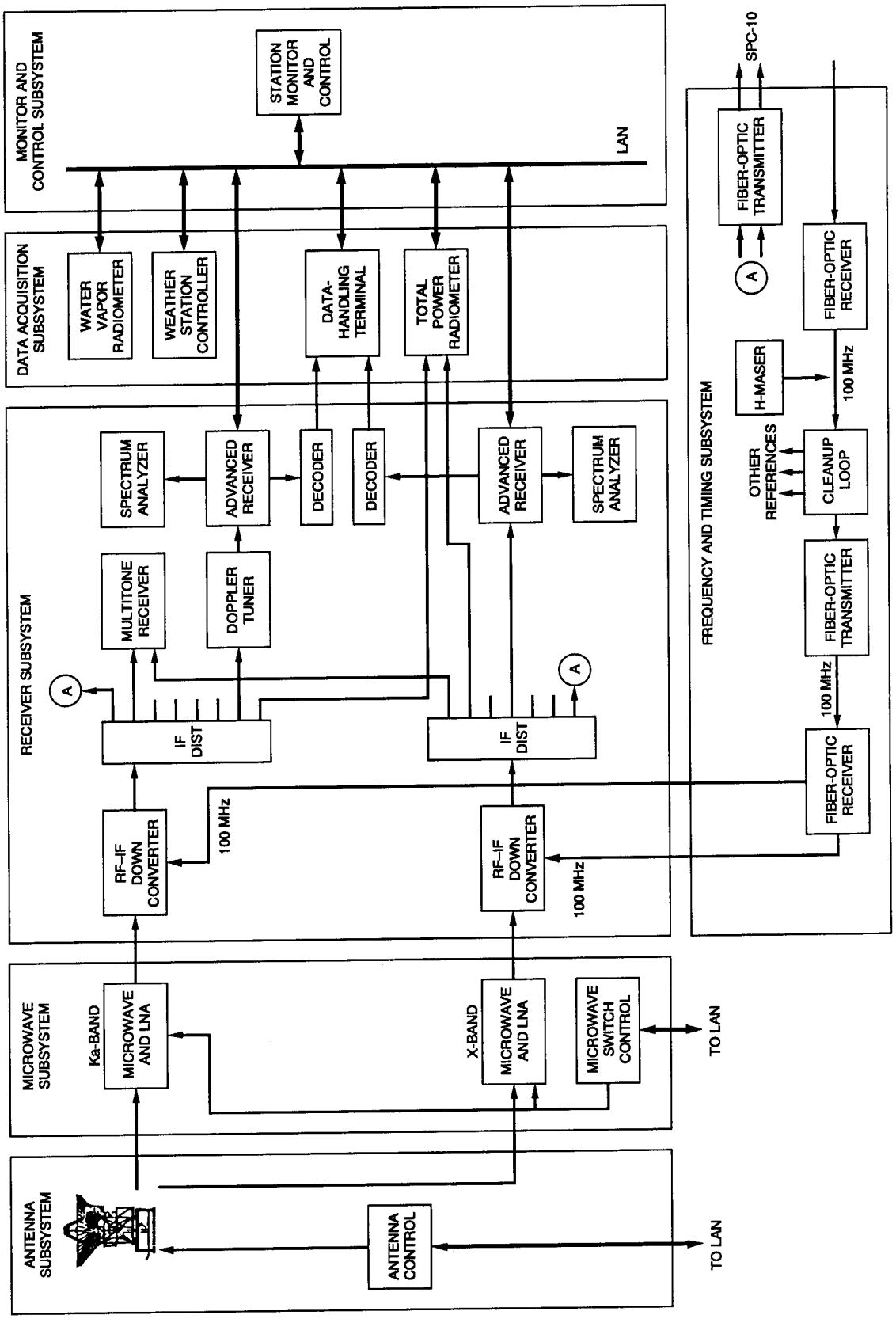

Fig. 6. KaBLE system installed at DSS 13.

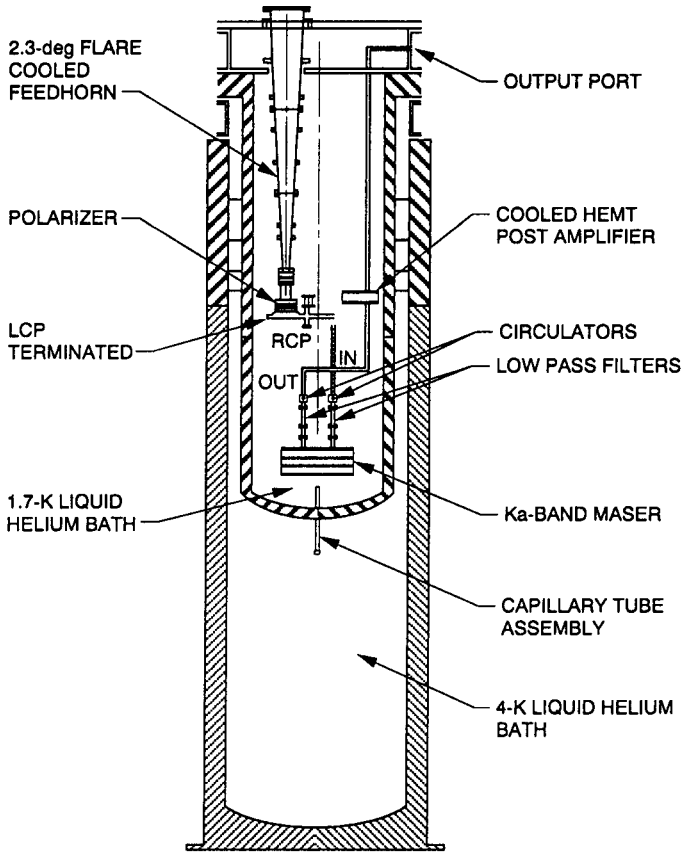

Fig. 7. Cross section of Ka-band maser cryostat, showing double-Dewar cryogenic system, cooled feedhorn, and maser.

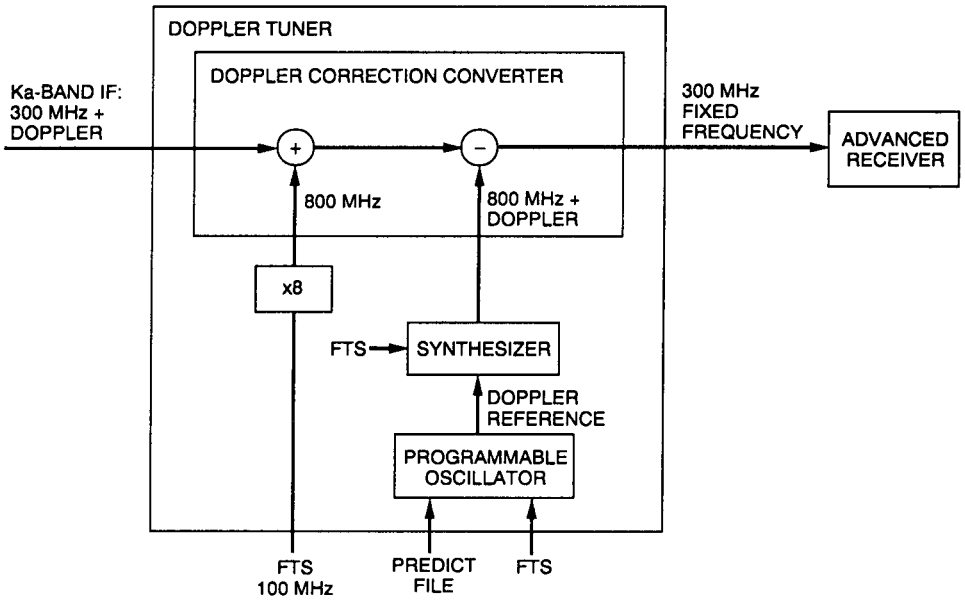

Fig. 8. Detail of KaBLE Doppler tuner.

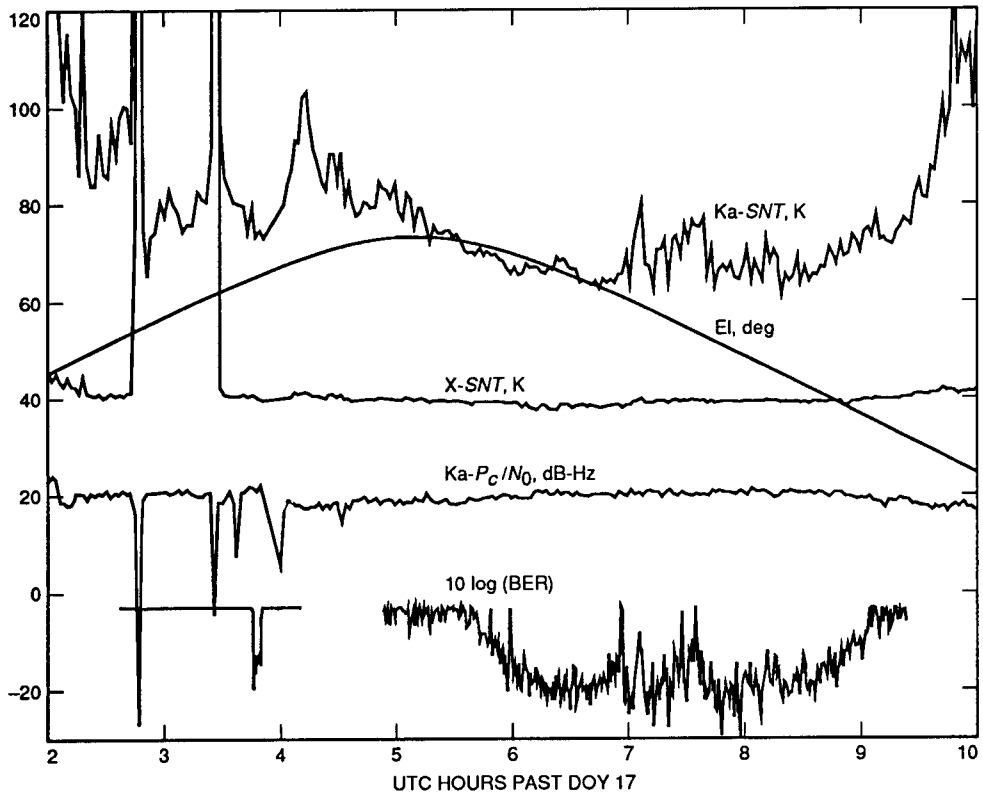

Fig. 9. Tracking statistics from DOY 17 of the telemetry demonstration showing carrier level, system noise temperature, elevation angle, and bit-error rate, indicating successful acquisition of telemetry data.

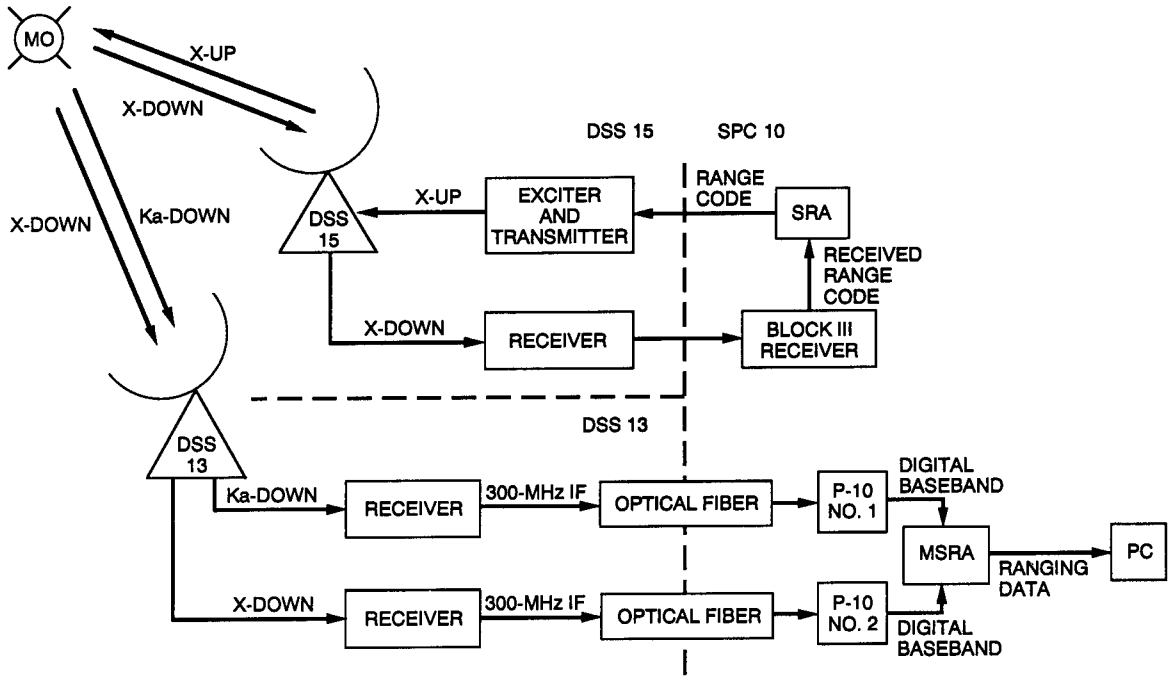

Fig. 10. Simplified diagram of test configuration used in the ranging demonstration.

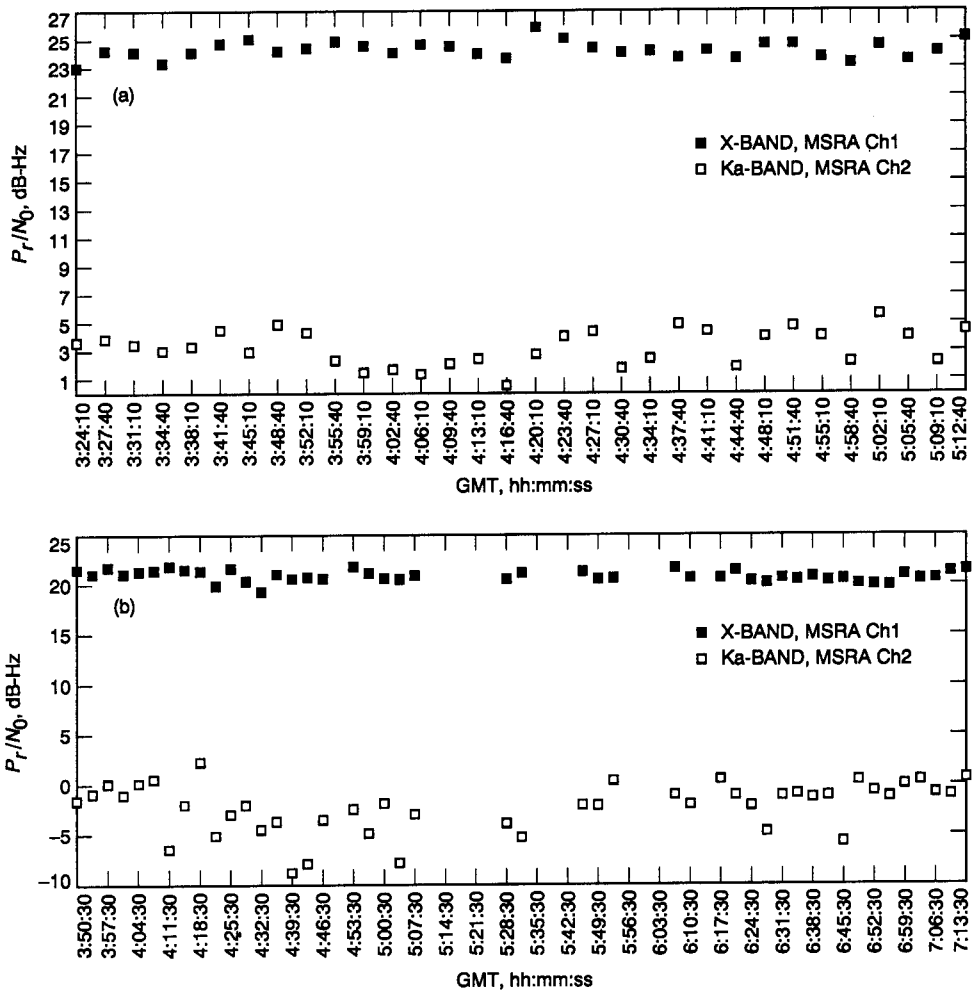

Fig. 11. Ranging SNR (P_r/N_0) received during two passes: (a) DOY 56 and (b) DOY 76.

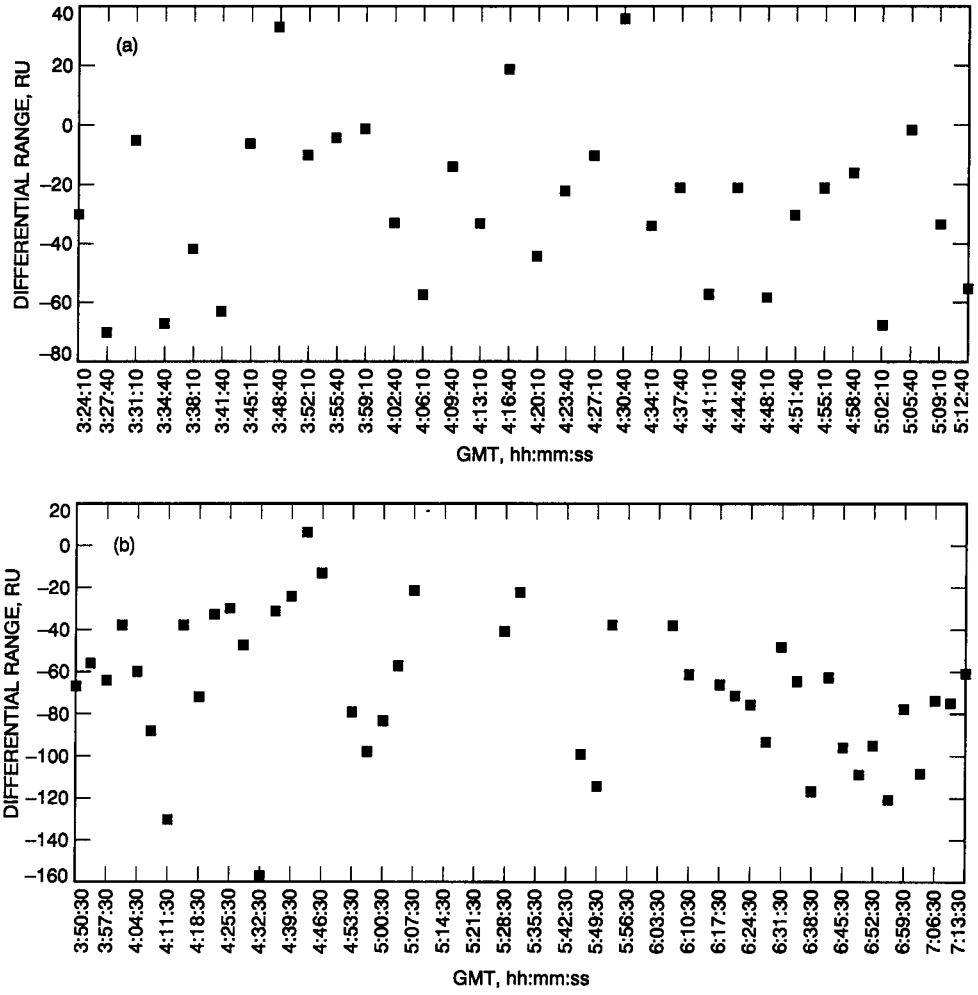

Fig. 12. X-/Ka-band differential range in RU of round-trip light time (1 RU ≈ 0.952 nsec): (a) DOY 56 and (b) DOY 76.

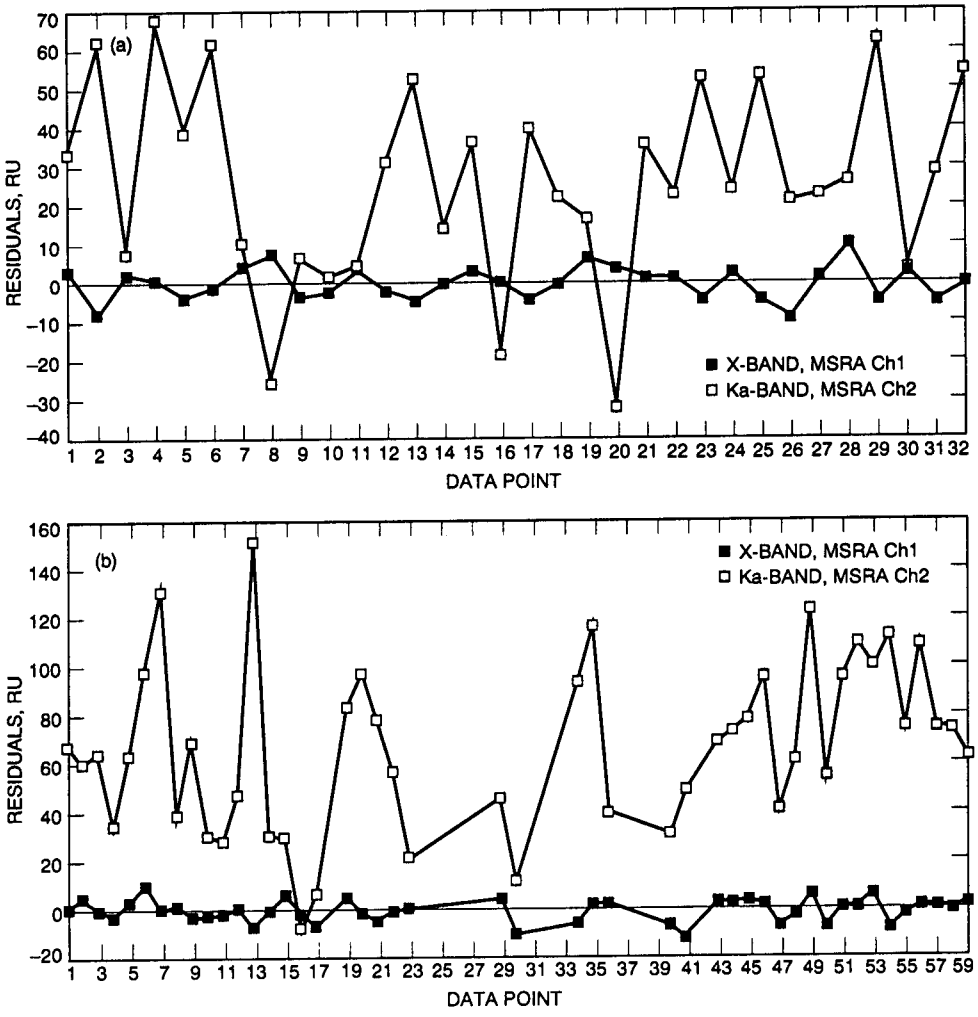

Fig. 13. X- and Ka-band residual range (after curve fitting to X-band data) showing increased scatter in the Ka-band data: (a) DOY 56 and (b) DOY 76.

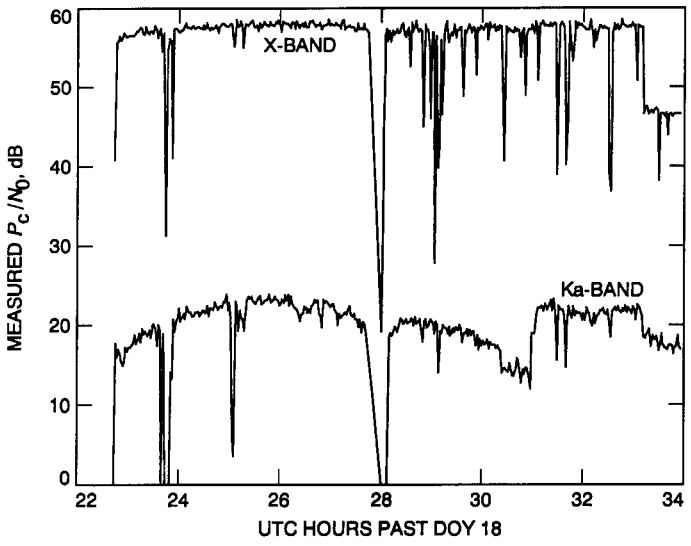

Fig. 14. Received carrier power during DOY 18 track showing dropouts in X- and Ka-band power due to uplink cycle slips and a large roll-off in Ka-band power beginning at 26:00 hr due to antenna mispointing and rain.

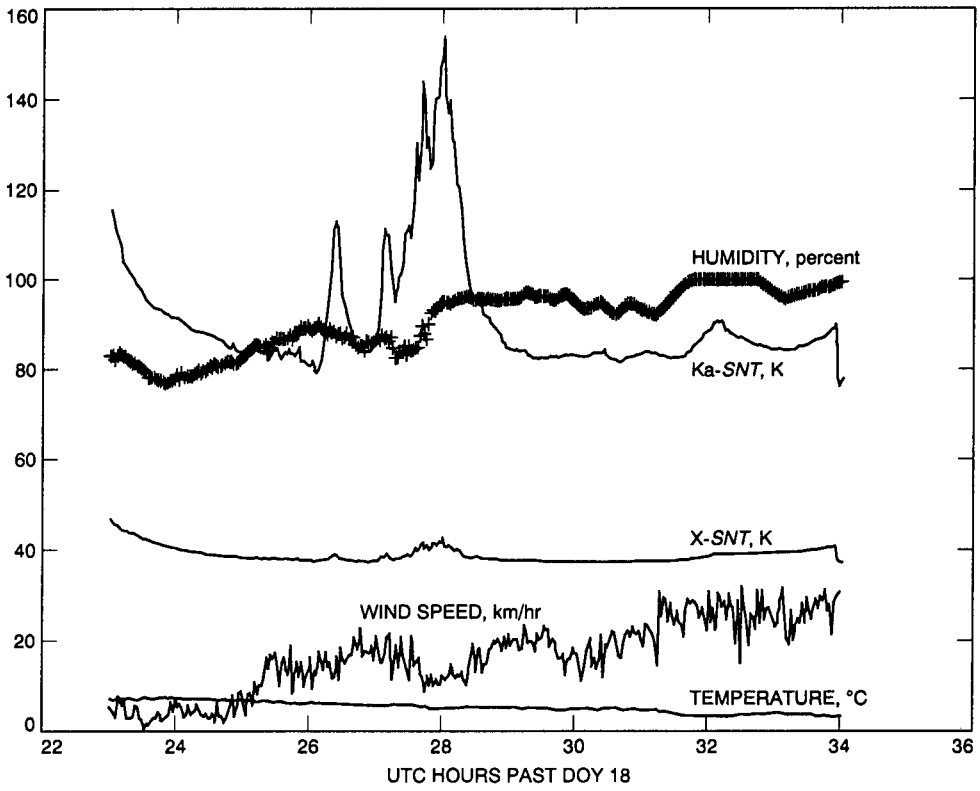

Fig. 15. System noise temperature and weather statistics for DOY 18 track showing rain signature in Ka-band noise temperature.

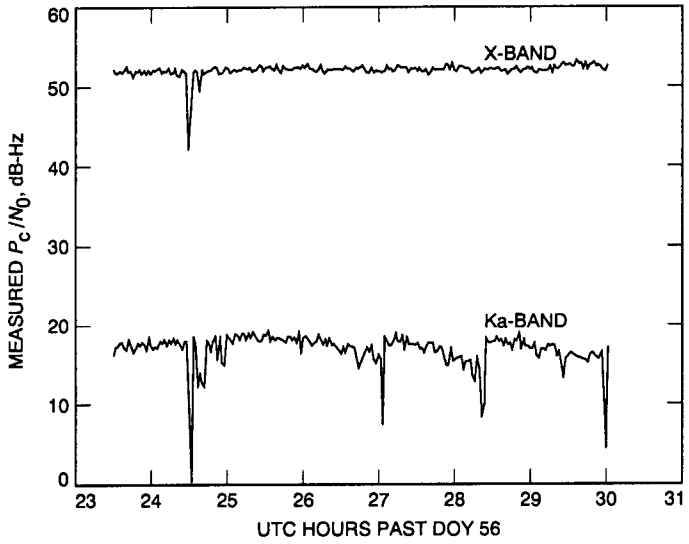

Fig. 16. Received carrier power during DOY 56 track showing accumulation of Ka-band pointing loss between boresights.

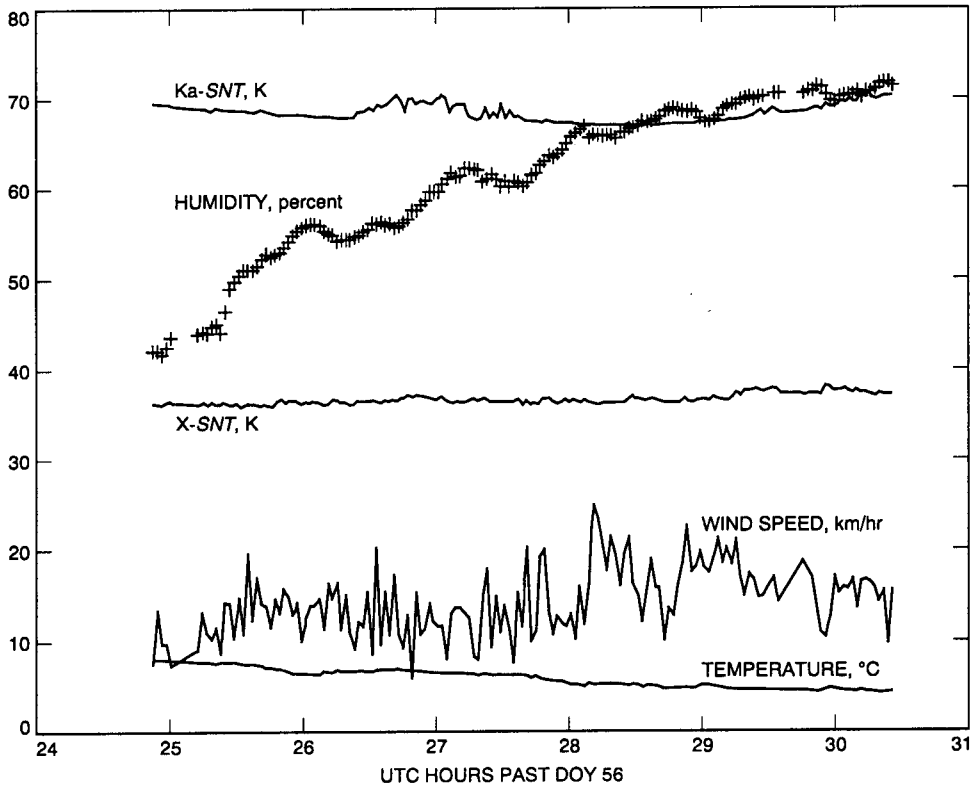

Fig. 17. System noise temperature and weather statistics for DOY 56 track, showing high Ka-band SNT due to HEMT.

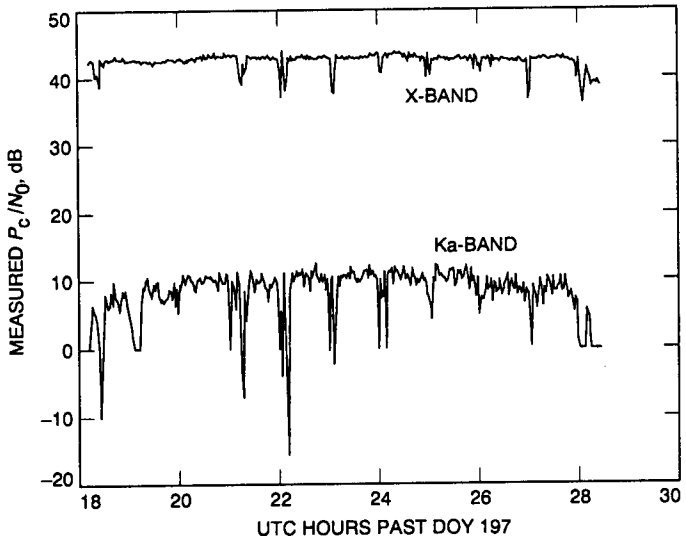

Fig. 18. Received carrier power for DOY 197 track with downward spikes showing hourly minicalibrations and boresights.

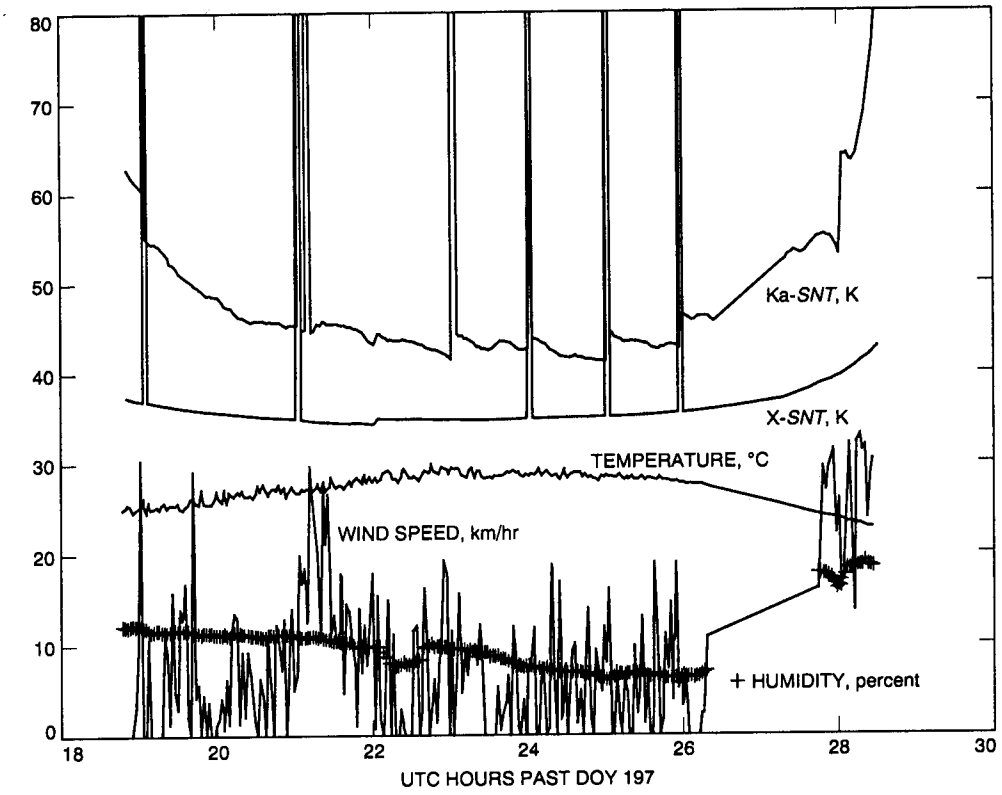

Fig. 19. System noise temperature and tracking statistics for DOY 197 track, showing fluctuations in Ka-band noise temperature due to gain instability.

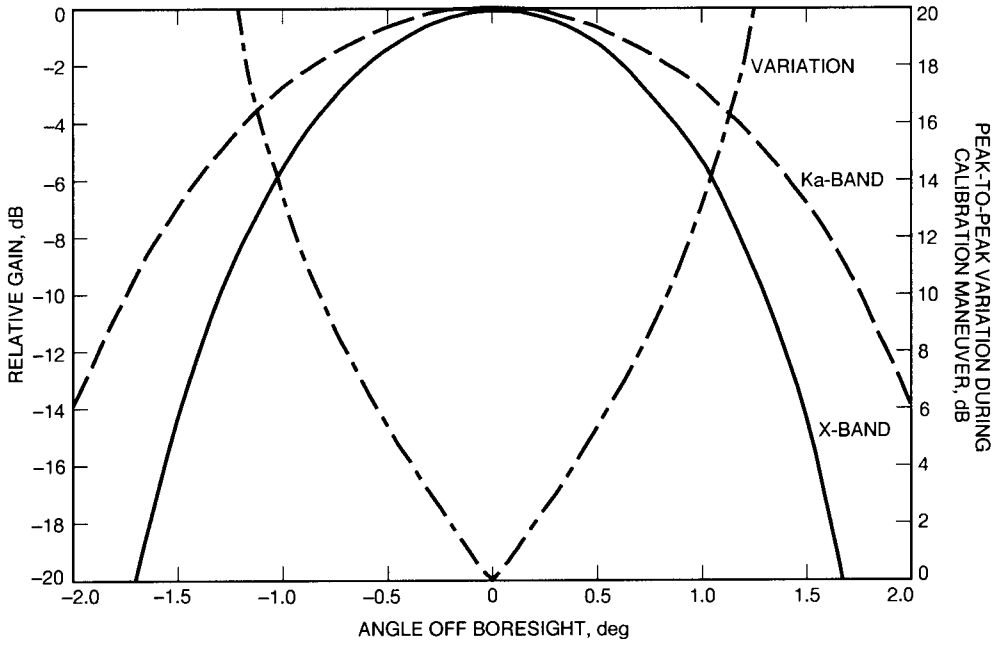

Fig. 20. X- and Ka-band HGA gain with expected variation in X-band power during calibration maneuver, as a function of pointing error.

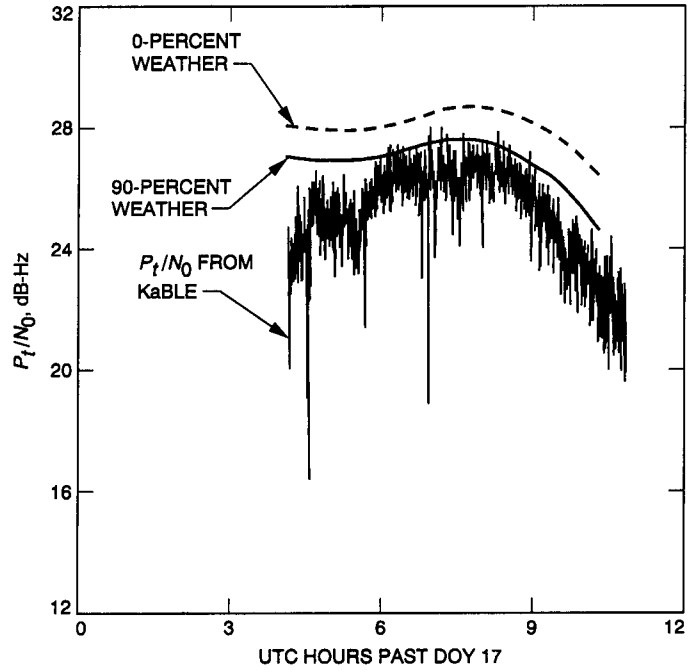

Fig. 21. Ka-band received SNR (P_t/N_0) compared with expectation based on modeled DSS-13 antenna performance.

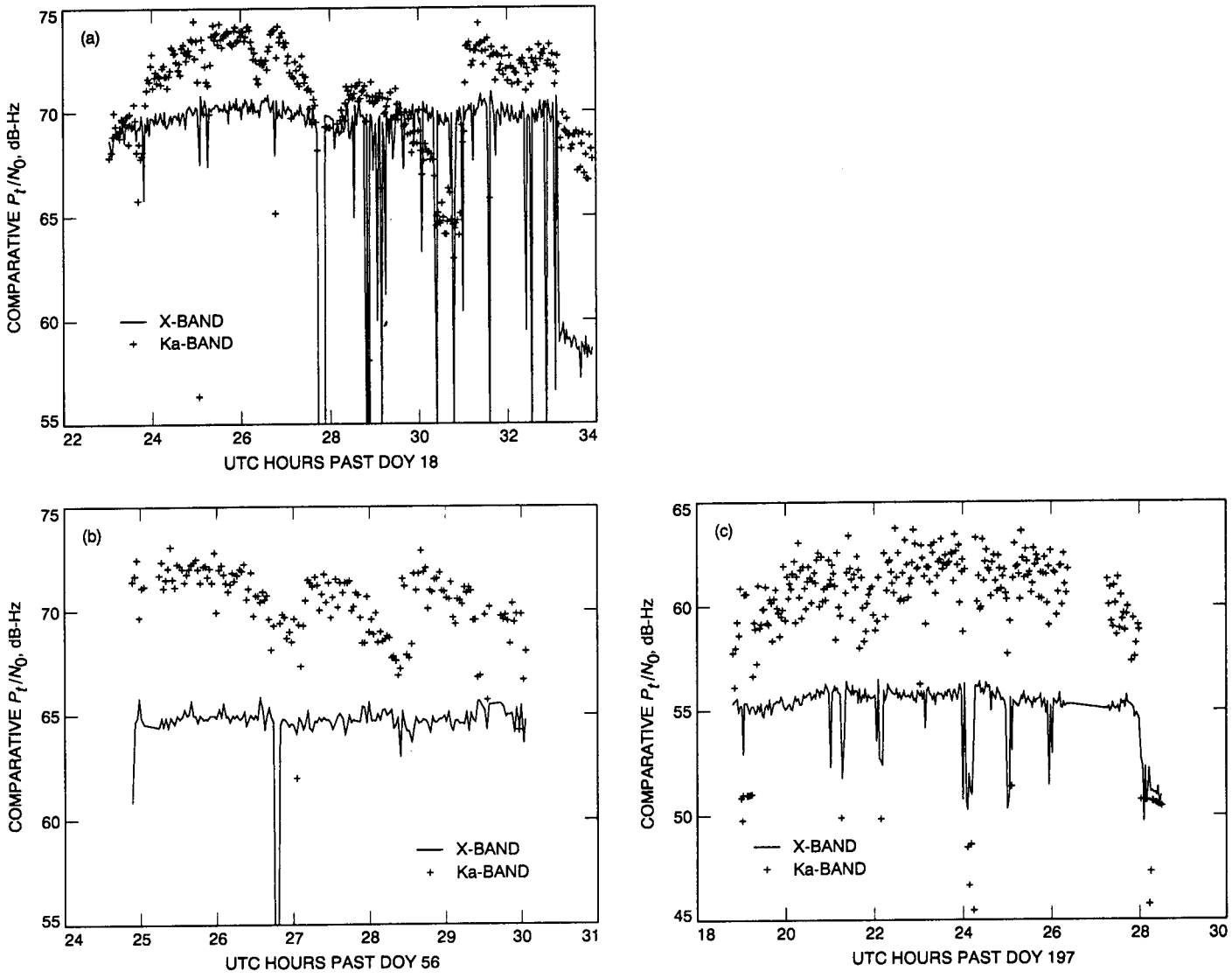

Fig. 22. Normalized X- and Ka-band SNR (P_t/N_0) for (a) DOY 18; (b) DOY 56; and (c) DOY 197, showing performance advantage of Ka-band over X-band at DSS 13, assuming identical spacecraft transmitter power and antenna size, as well as optimized X- and Ka-band receiver noise temperature (see VI.D.3). Scatter in Ka-band data is high due to weak (7 to 12 dB-Hz) signal strength.